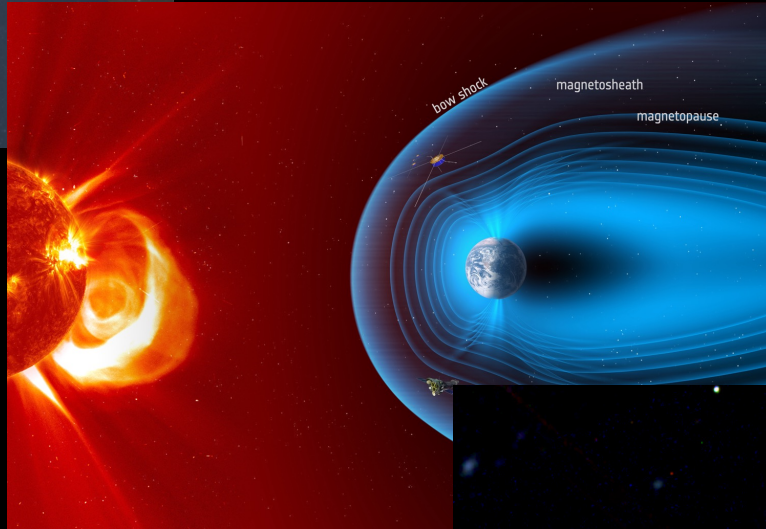
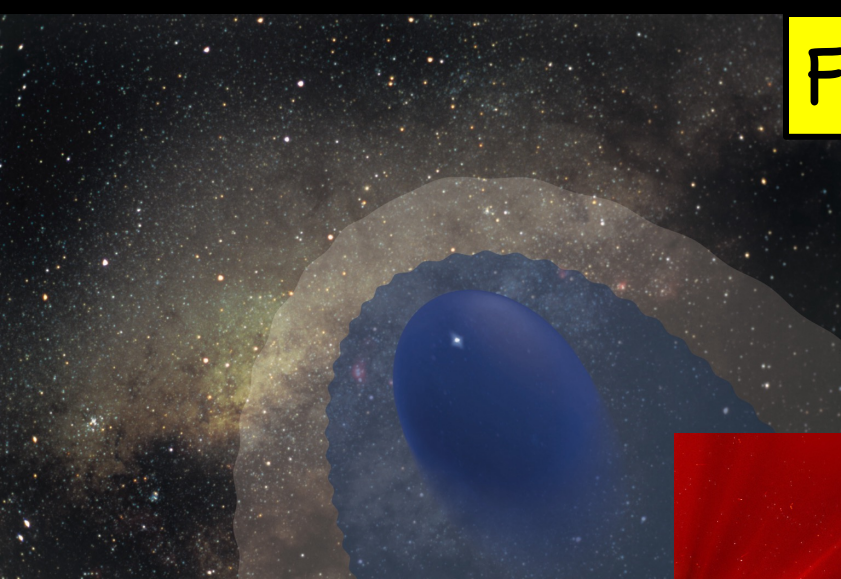


From CX to SWCX to CXU

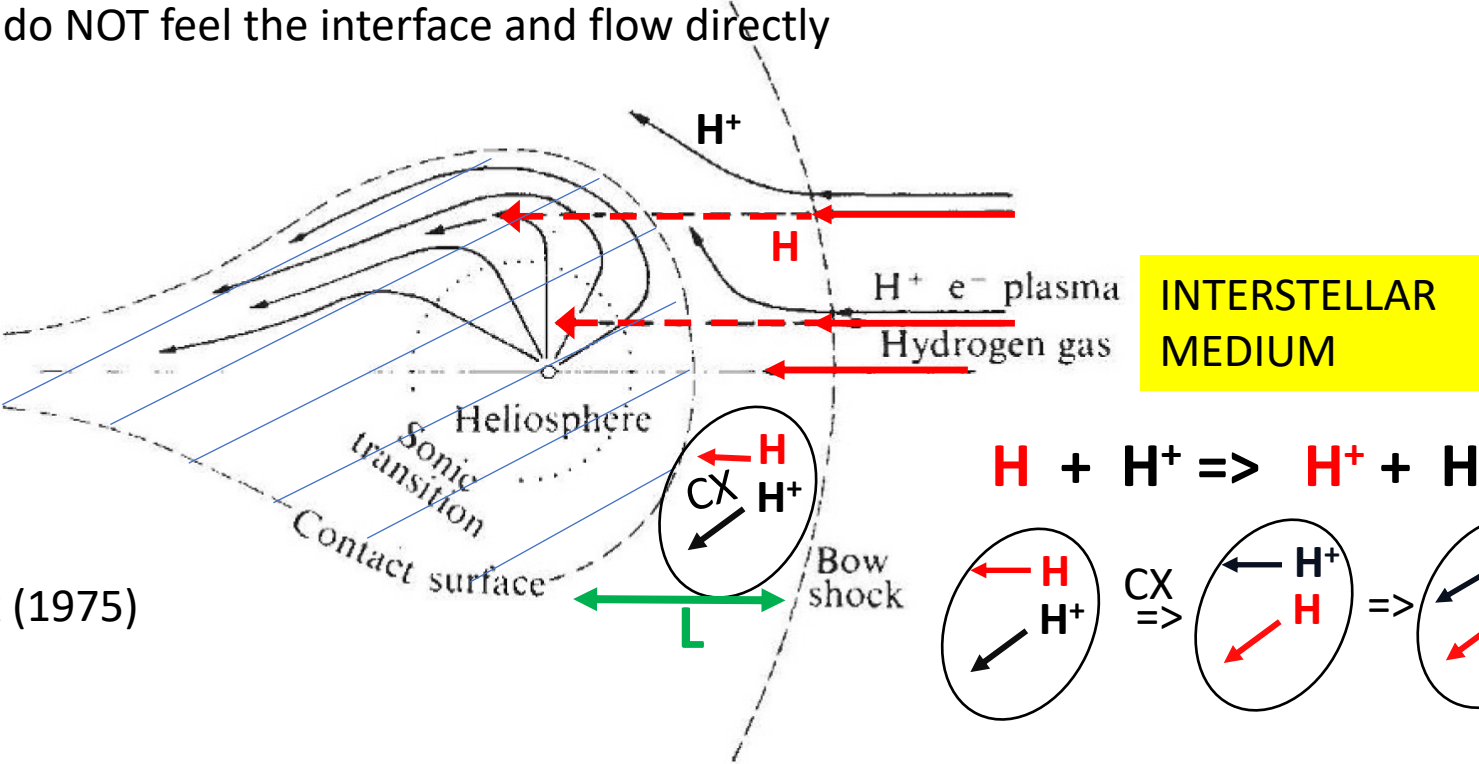
R. Lallement / GEPI, Obs. Paris, PSL*





H - H⁺ CX SHAPES THE HELIOSPHERE

Sun in partly ionized cloud; H⁺, e⁻ start to be deflected and surround the heliosphere ;
Neutrals do NOT feel the interface and flow directly



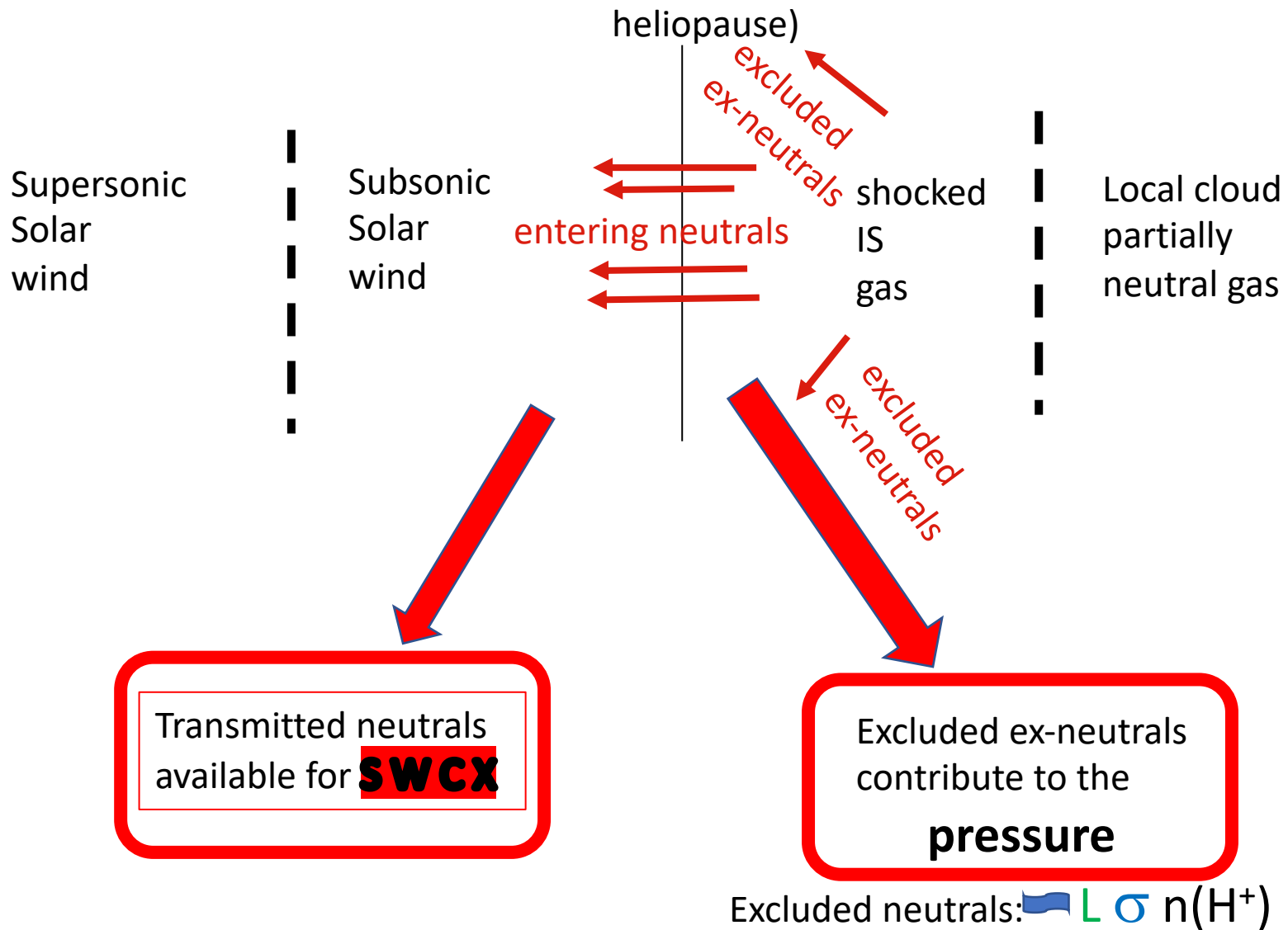
Wallis, Max (1975)

H-H⁺ charge-exchange=> H and H⁺ exchange their momentum

=> the « new » H⁺ is advected in the plasma flow, the « new » H gets the deviation of the proton

Affected neutrals: $L \sigma n(H^+)$ => a fraction of neutrals are not entering the heliosphere

Note: Chevalier and Raymond (1978) also started to model H-H⁺ CX to explain H α lines in SNRs



If L or $n(H^+)$ are large enough for $L \sigma n(H^+) > 1$ all neutrals are coupled to the plasma and do not enter the fully ionized gas => a **mono-fluid** model is appropriate

If $L \sigma n(H^+) < 1$ a fraction of neutrals enters the fully ionized gas, **two-fluid** models are needed

Influence of CX on size and shape of the heliosphere

Baranov, Malama, 1993

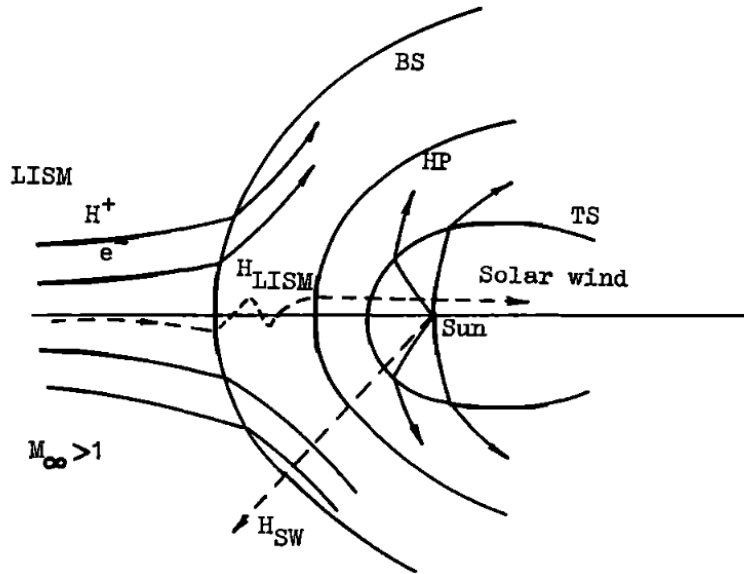


Fig. 1. Qualitative picture of the solar wind interaction with the LISM: BS is the bow shock, HP is the heliopause, TS is the termination (inner) shock; H_{LISM} are H atoms of the LISM's origin, H_{SW} are energetic H atoms of the solar wind origin (neutral solar wind).

Self-consistent

-HD model for the plasma

-Kinetic mode for the neutrals

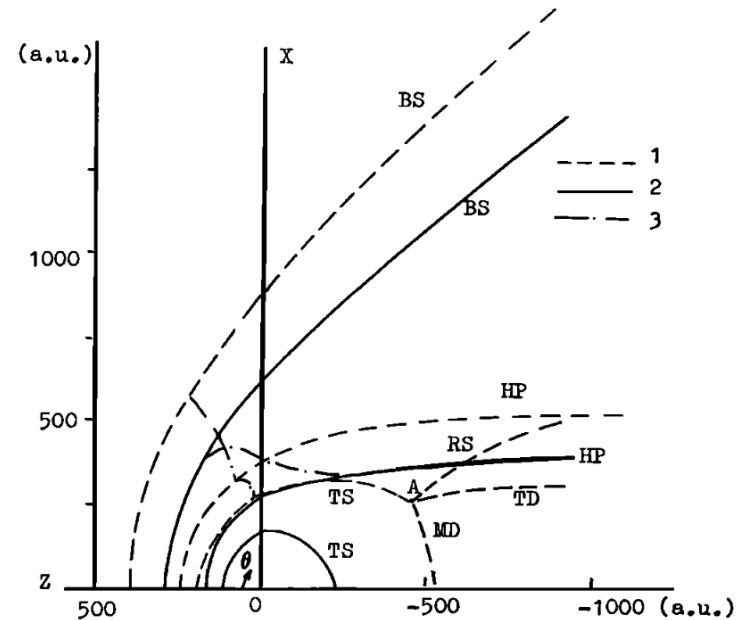
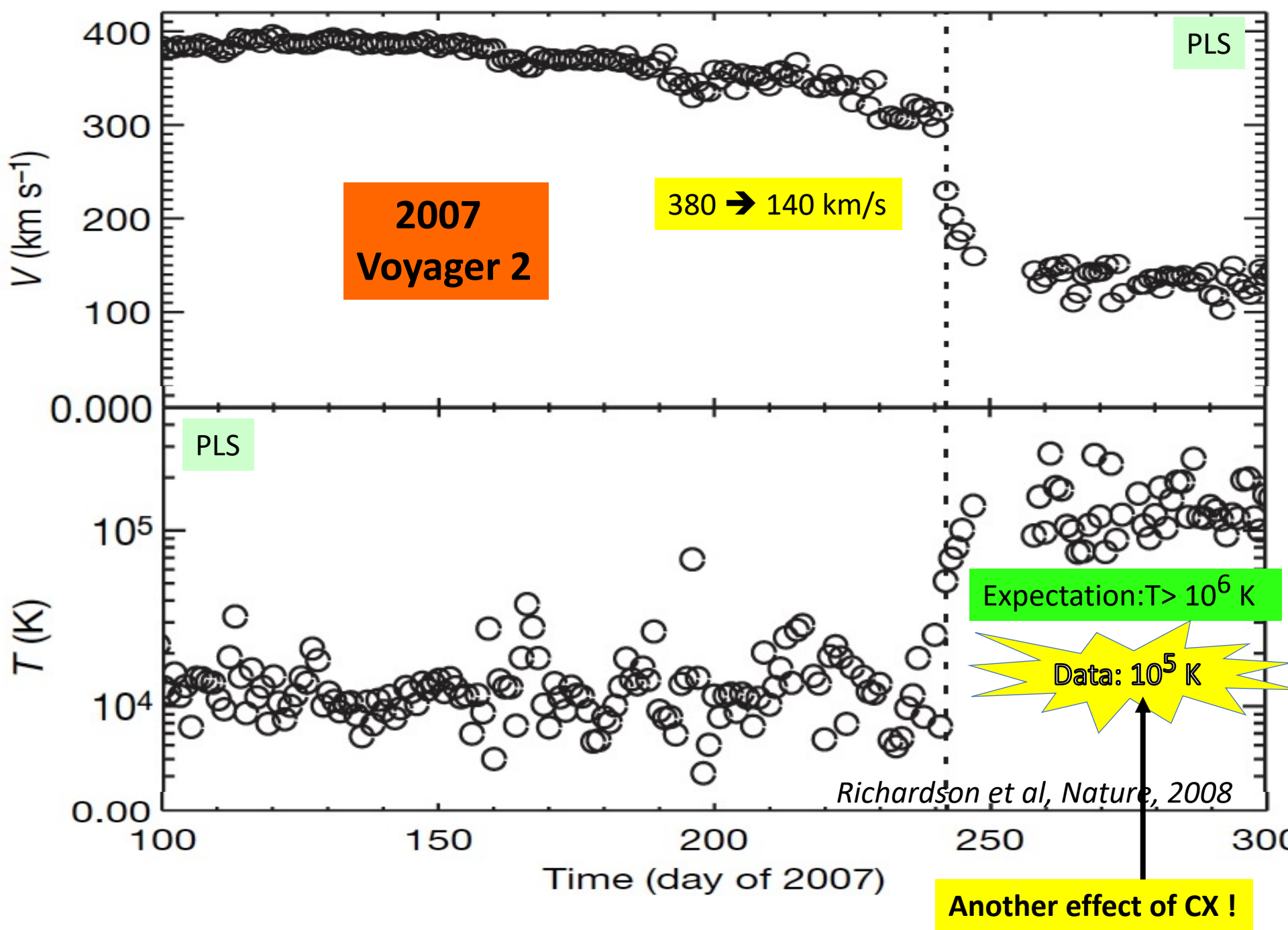
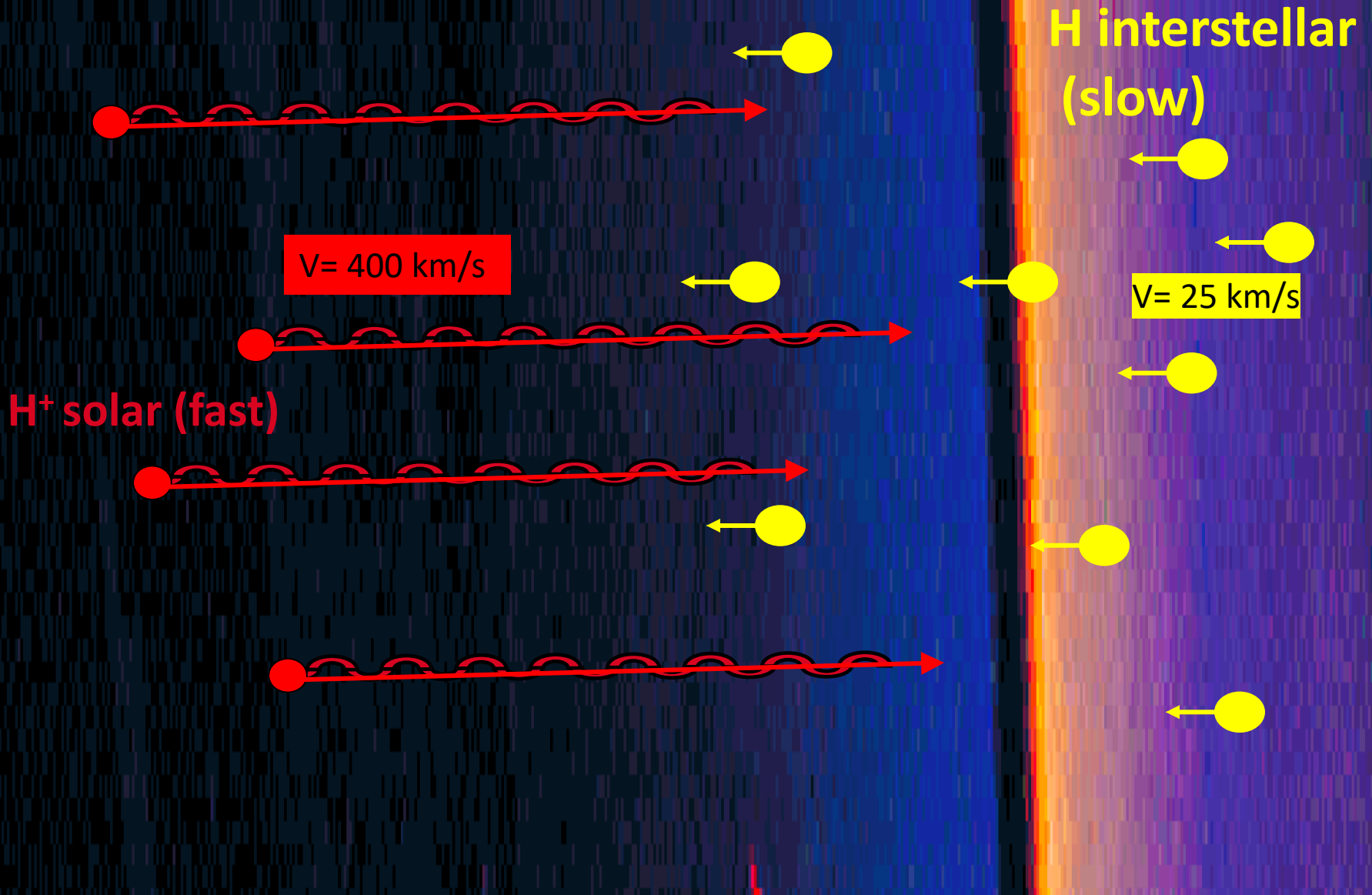


Fig. 2. Geometrical pattern of the interface. Results of the numerical calculations for $n_{H_{\infty}} = 0$ (1) and $n_{H_{\infty}} = 0.14 \text{ cm}^{-3}$ (2); curves (3) are the sonic lines. Positions of bow shock (BS), termination shock (TS), heliopause (HP), reflected shock (RS), tangential discontinuity (TD), and Mach disc (MD) are shown.

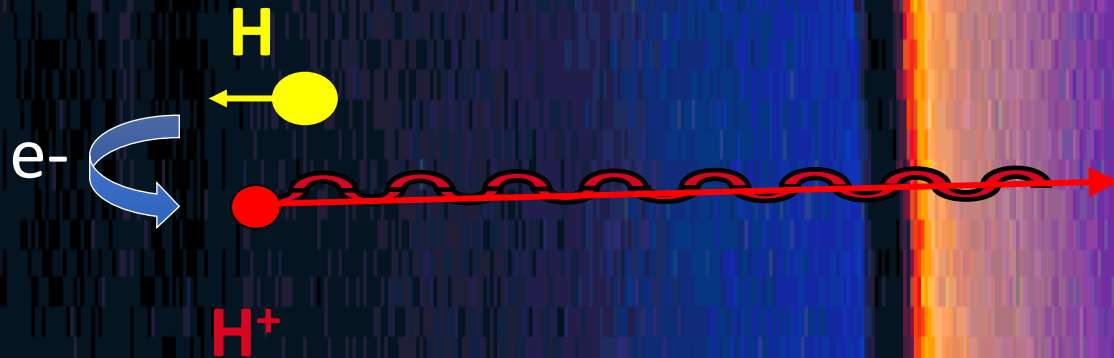
The heliopause and the solar wind termination shock get closer to the Sun !



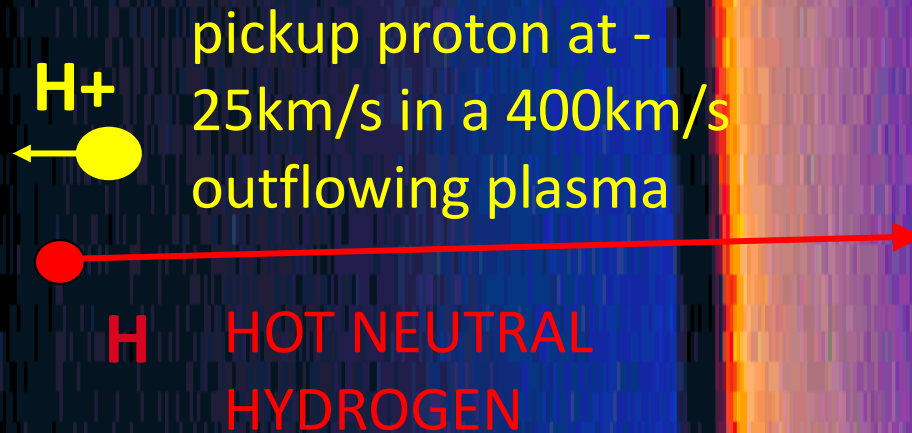
Charge exchange in the supersonic SW
(mainly $\text{H} + \text{H}^+ \rightarrow \text{H}^+ + \text{H}$)



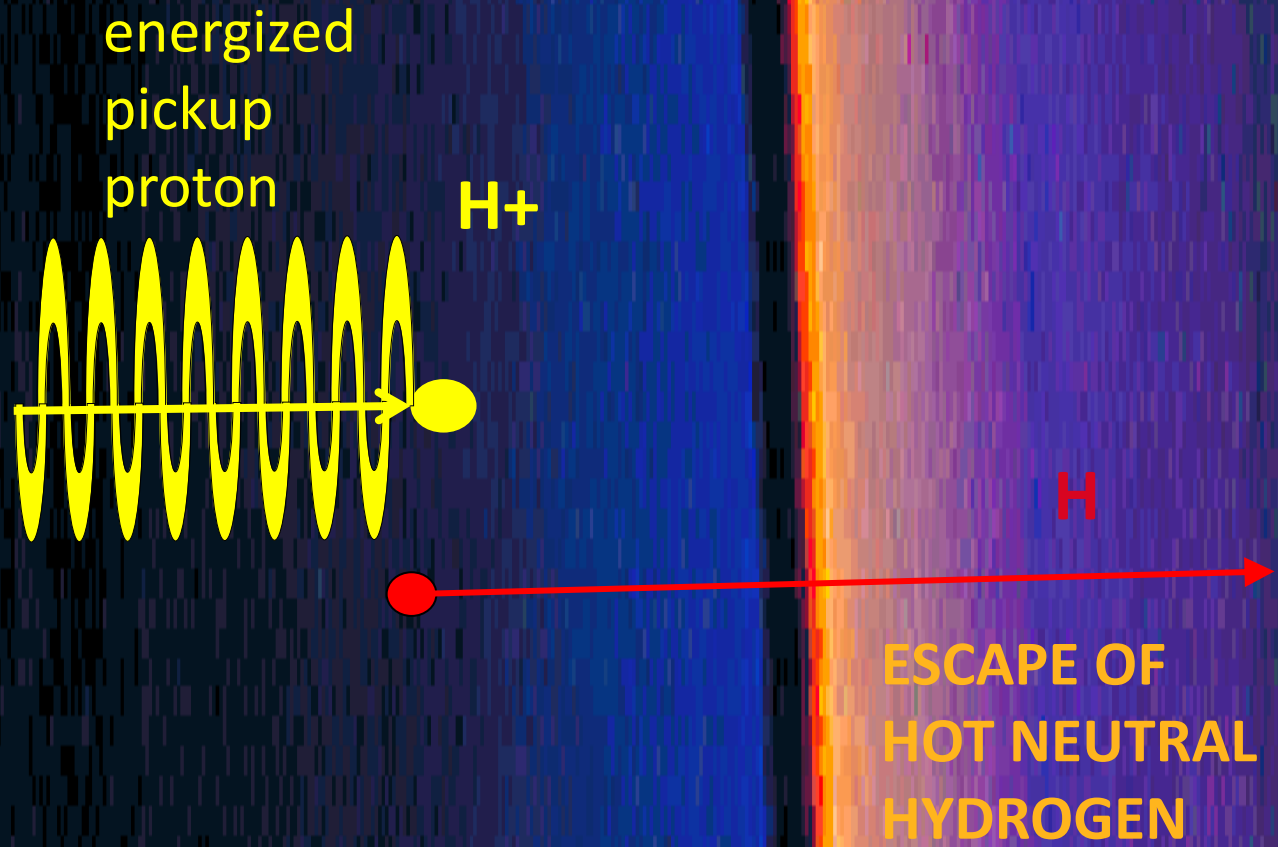
Charge exchange: mainly $\text{H} + \text{H}^+ \rightarrow \text{H}^+ + \text{H}$

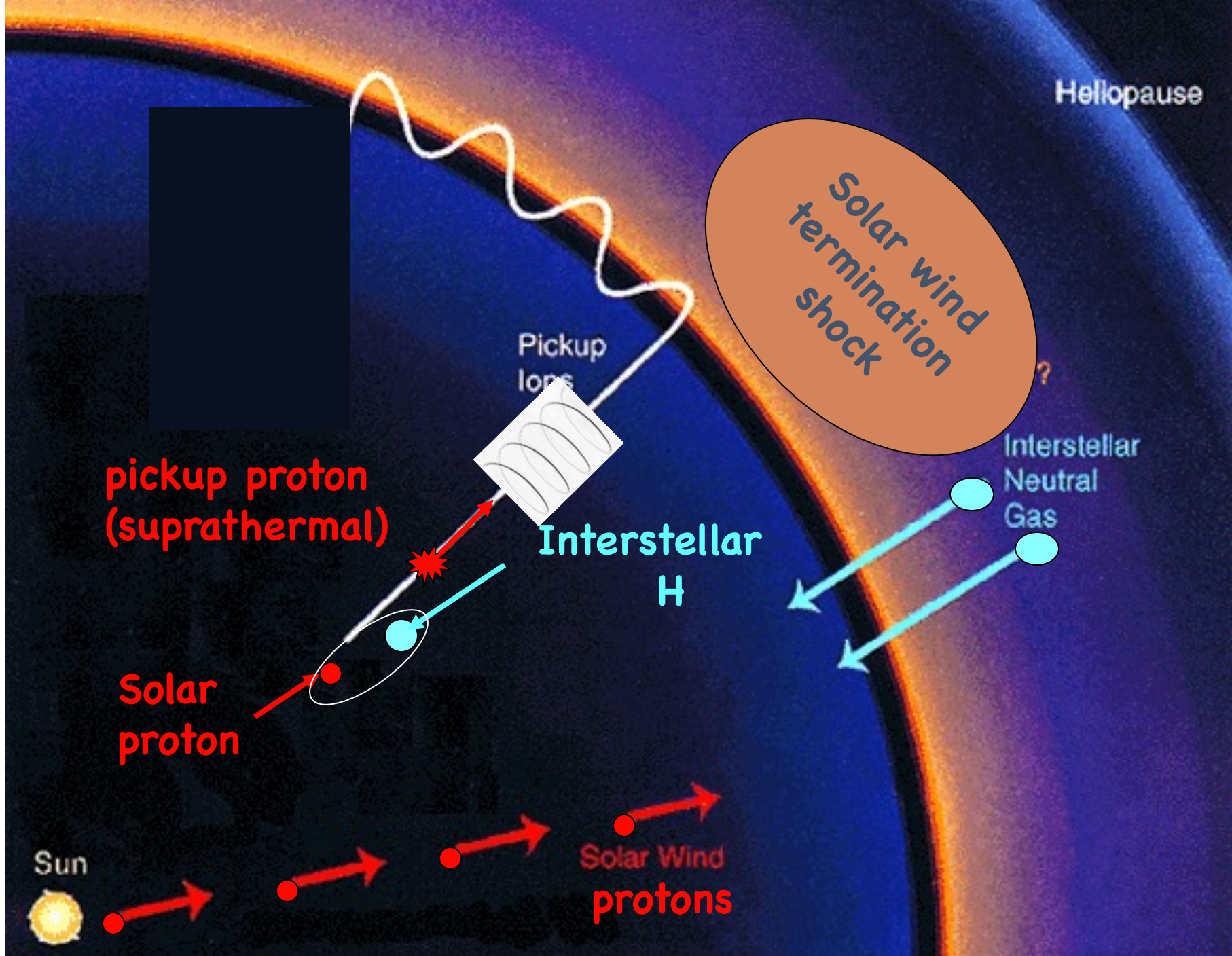


Right after charge exchange



Charge exchange consequences





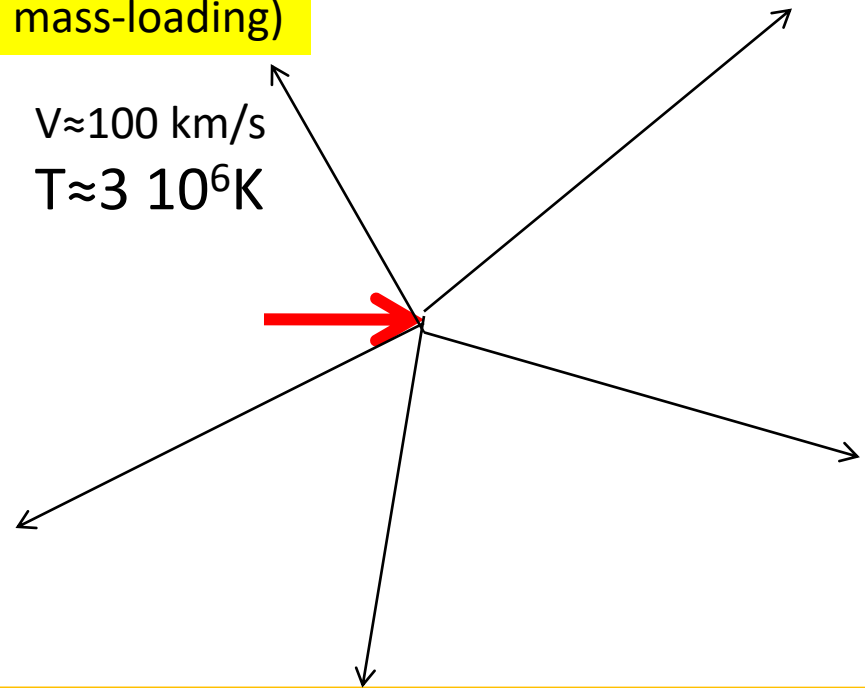
WITHOUT pickup ions (no mass-loading)

Solar wind: 400 km/s

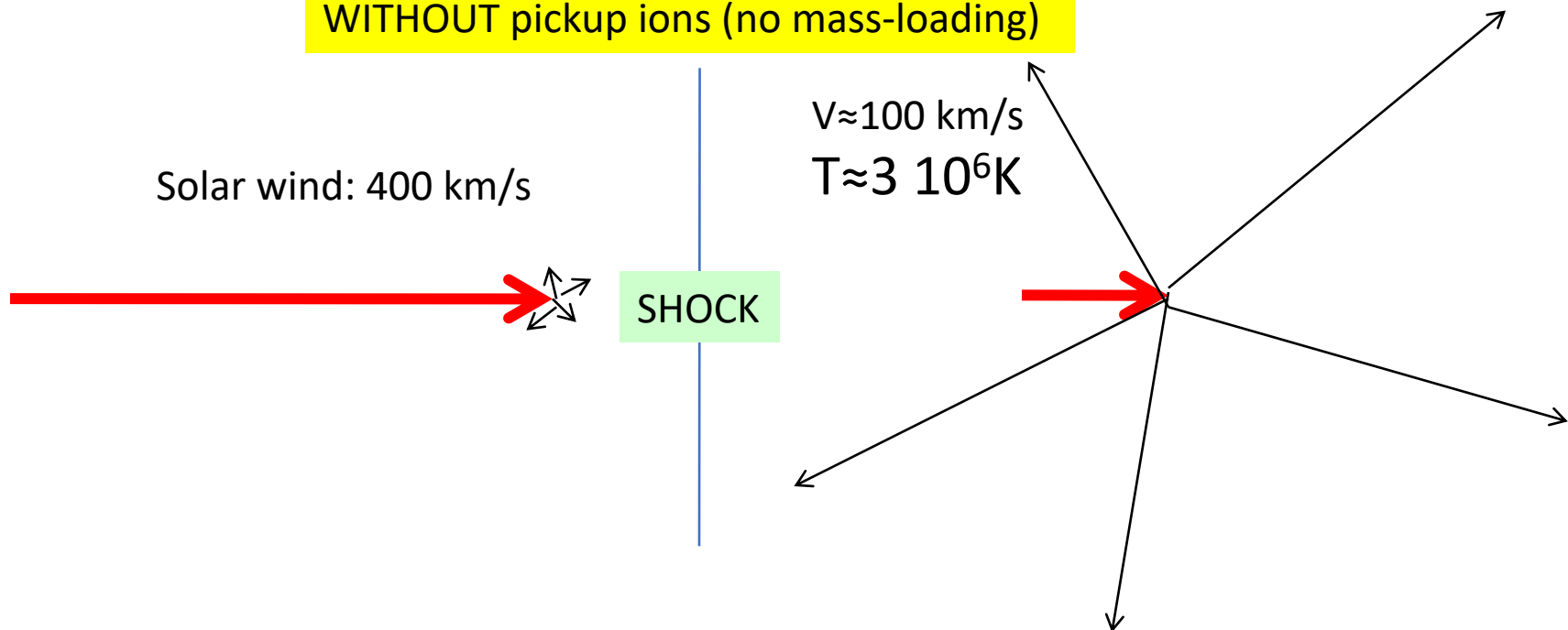


SHOCK

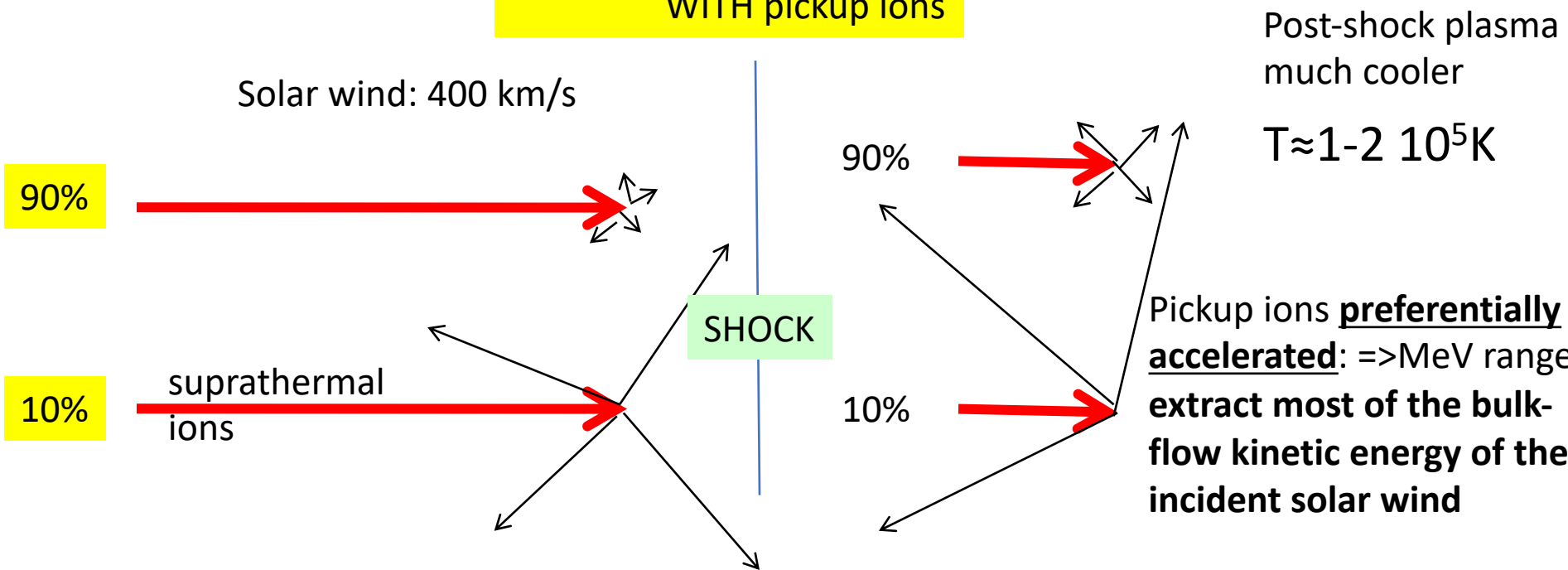
$V \approx 100 \text{ km/s}$
 $T \approx 3 \cdot 10^6 \text{ K}$



WITHOUT pickup ions (no mass-loading)



WITH pickup ions



Conclusions:

The influences of the H-H⁺ (or He-H⁺, He, He⁺) CX reactions are very different
-depending on **densities**, relative **velocities** (through fluxes and cross-section values),

-depending on sizes of interfaces relative to the volumes of interacting media
=> complex, multi-fluid models are sometime needed

- **Pickup ions** may also have a significant role on the structure of the interface

Until 1996, no mentions of charge-exchange between interstellar neutrals and solar wind high ions !!



Yuji Hyakutake en compagnie de ses jumelles Fujinon 25x150



And along came Hyakutake, blazing away ...

Cox, D, 1998

50 years after the discovery of the solar wind due to comets (Biermann 1951), a comet again is at the origin of a new discovery: solar wind charge-exchange X-ray (SWCX)

FIRST X-RAY IMAGE OF A COMET
Comet Hyakutake · C/1996 B2 ROSAT HRI
March 27, 1996

nucleus + → Sun

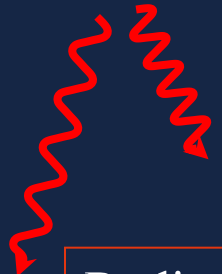
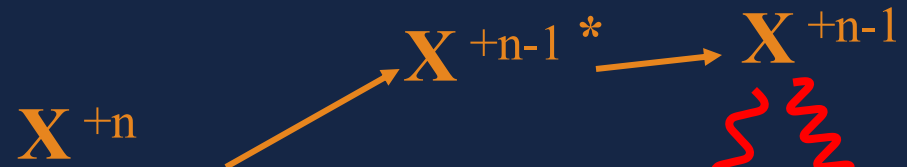
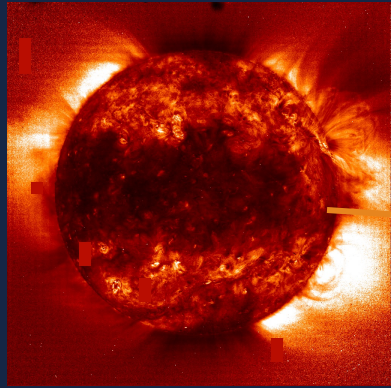
10 arcmin
55 000 km

comet motion

C. Lisse, M. Mumma, NASA GSFC
K. Dennerl, J. Schmitt, J. Englhauser, MPE

SOLAR WIND HIGHLY CHARGED IONS,
FROM THE 1-2 MK CORONA

CHARGE STATE « FROZEN » in INTERPLANETARY SPACE



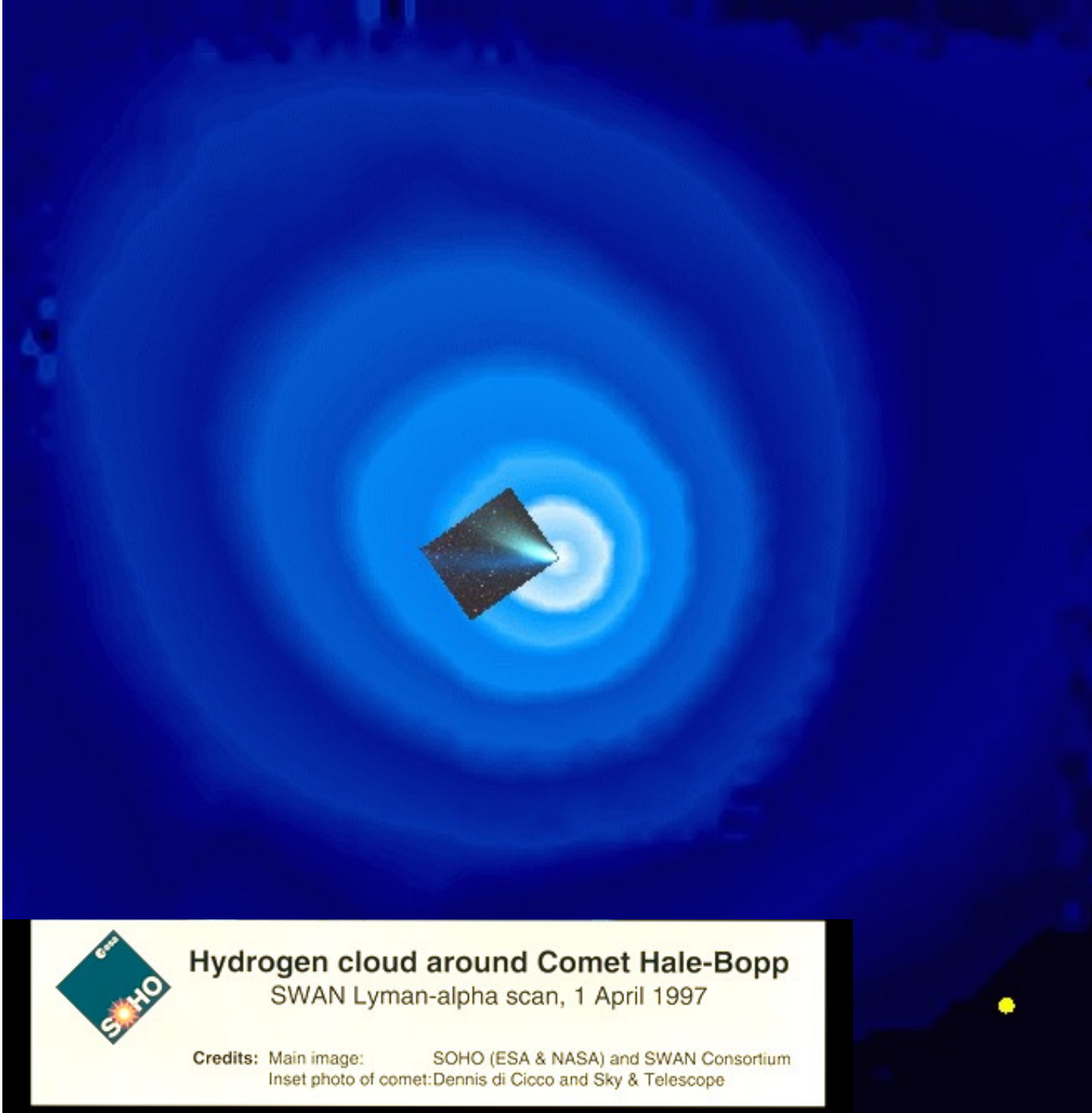
Radiative cascade

Atoms or Molecules
Outgassed by the comet

M
Electronic capture



Mechanism devised by Cravens, 1997 (Geophys. Res. Let.)



H₂O outgassed
by the comet
is rapidly
dissociated into
H and OH

H is scattering
the solar Ly- α
radiation



Hydrogen cloud around Comet Hale-Bopp

SWAN Lyman-alpha scan, 1 April 1997

Credits: Main image: SOHO (ESA & NASA) and SWAN Consortium
Inset photo of comet: Dennis di Cicco and Sky & Telescope

Main High Ions in the Solar Wind

C^{4+,5+,6+} N^{5+,6+,7+} O^{5+,6+,7+,8+} Ne^{8+,9+,10+}

Mg^{7+,8+,9+,10+} Si^{8+,9+,10+,11+} S^{10+,11+,12+,13+,14+} Fe^{9+,10+,11+,12+,13+,14+}

Higher charge states during episodic energetic events (solar flares) ==> e.g. Fe^{12+,13+,14+}, S^{12+,13+,14+}

Neutral populations to participate in CX

-origin: comets, planetary exospheres, IS gas
-H, He, H₂O, O

Parameters controlling the emission:

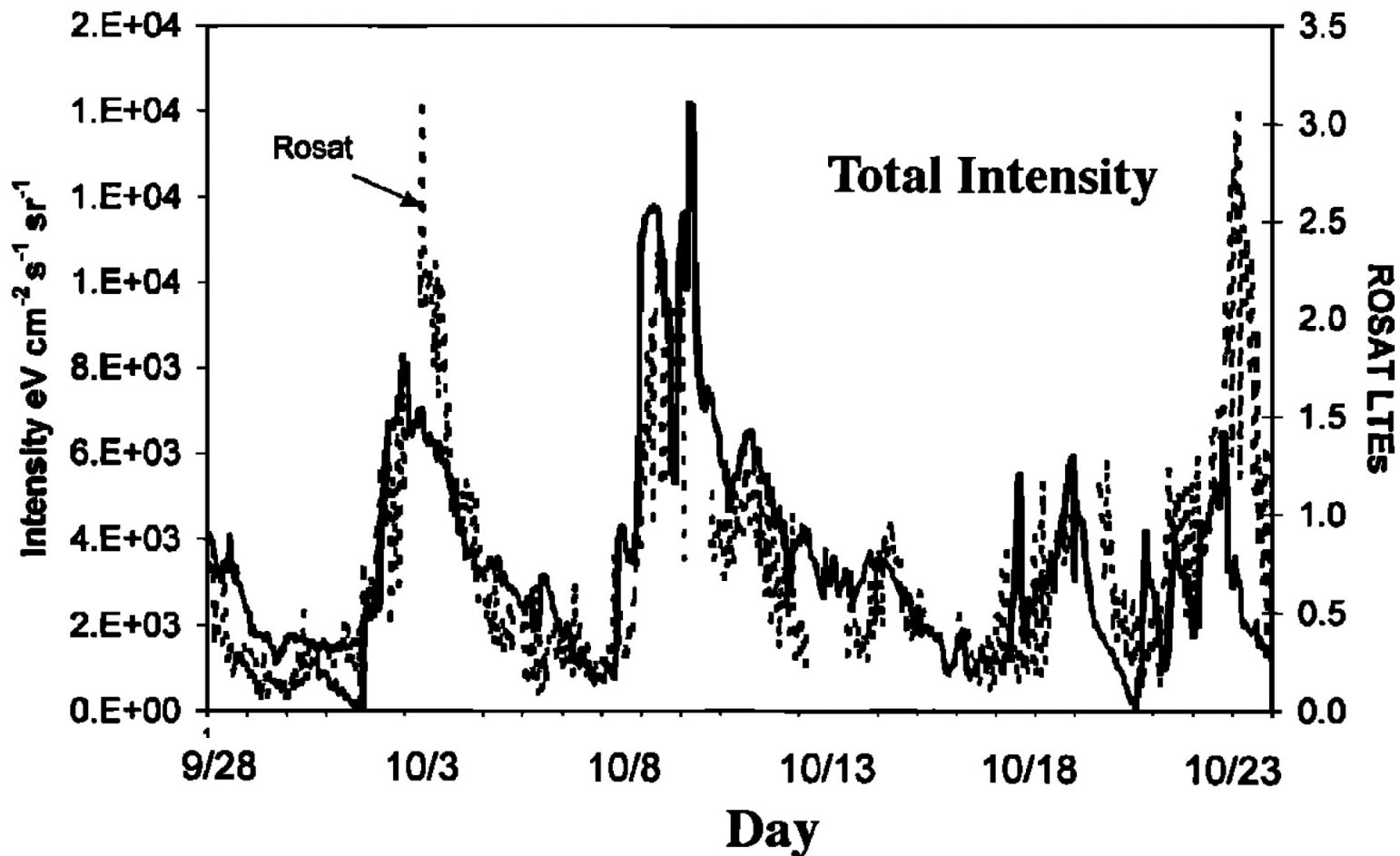
- Ion properties (solar activity, wind source region):
influence SW velocity, composition, charge state
- neutral density distributions
- Ion charge state-neutral cross sections (type, velocity)
- Radiative cascade probabilities

SWCX

A tool but also a foreground difficult to predict

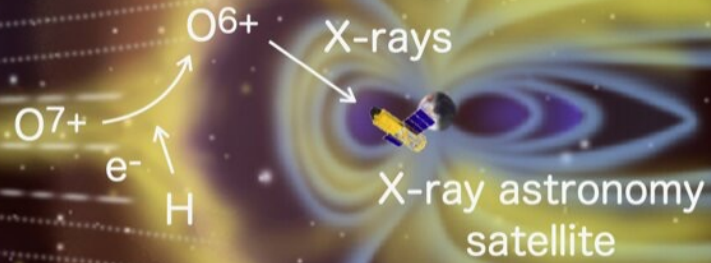
The « Long Term Enhancements » (LTEs) of the ROSAT data

The diffuse background intensity in a fixed direction varies with time



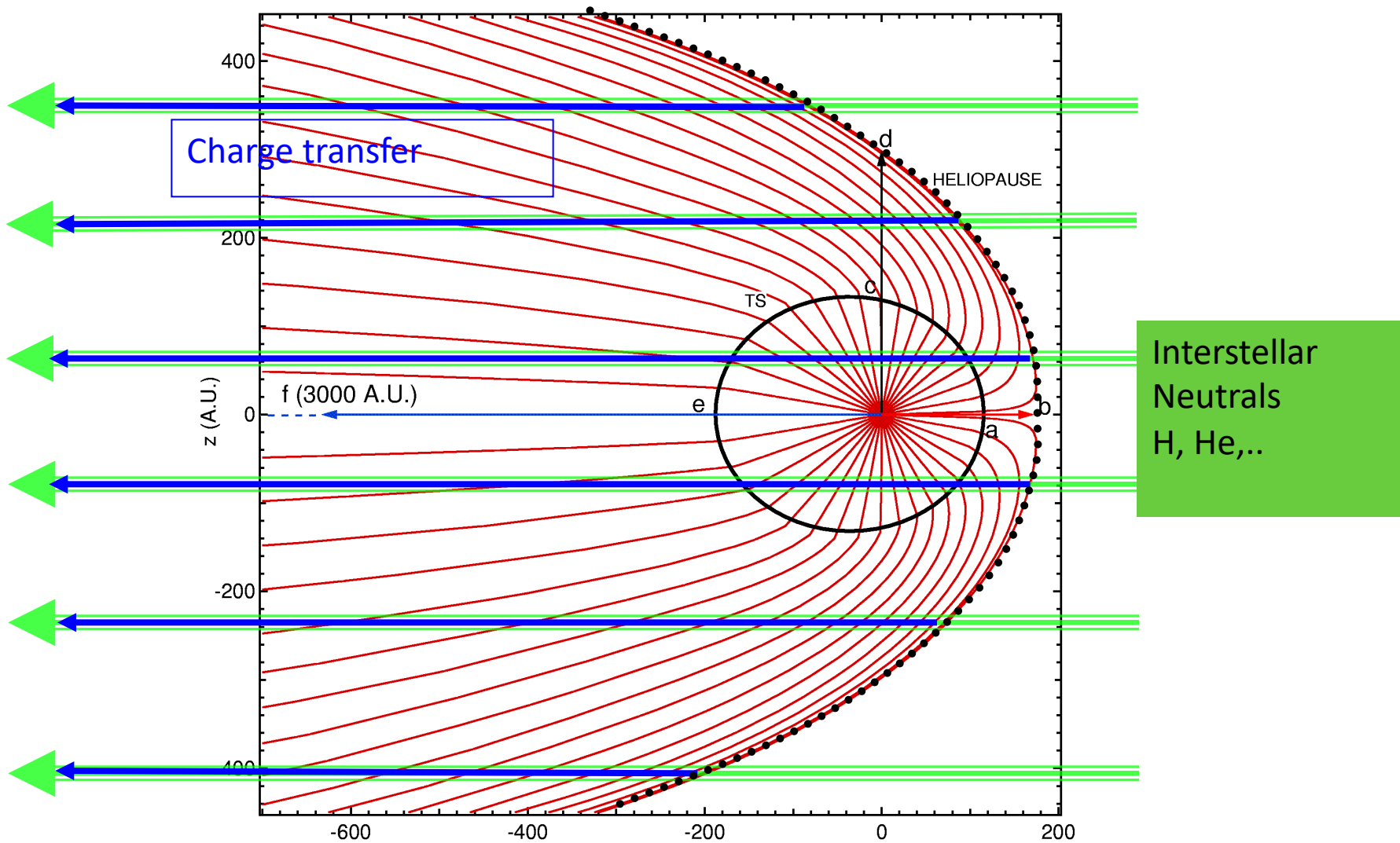
Timescales from minute to several days

charge exchange
e.g., $O^{7+} + H \rightarrow O^{6+} + H^+ + h\nu$



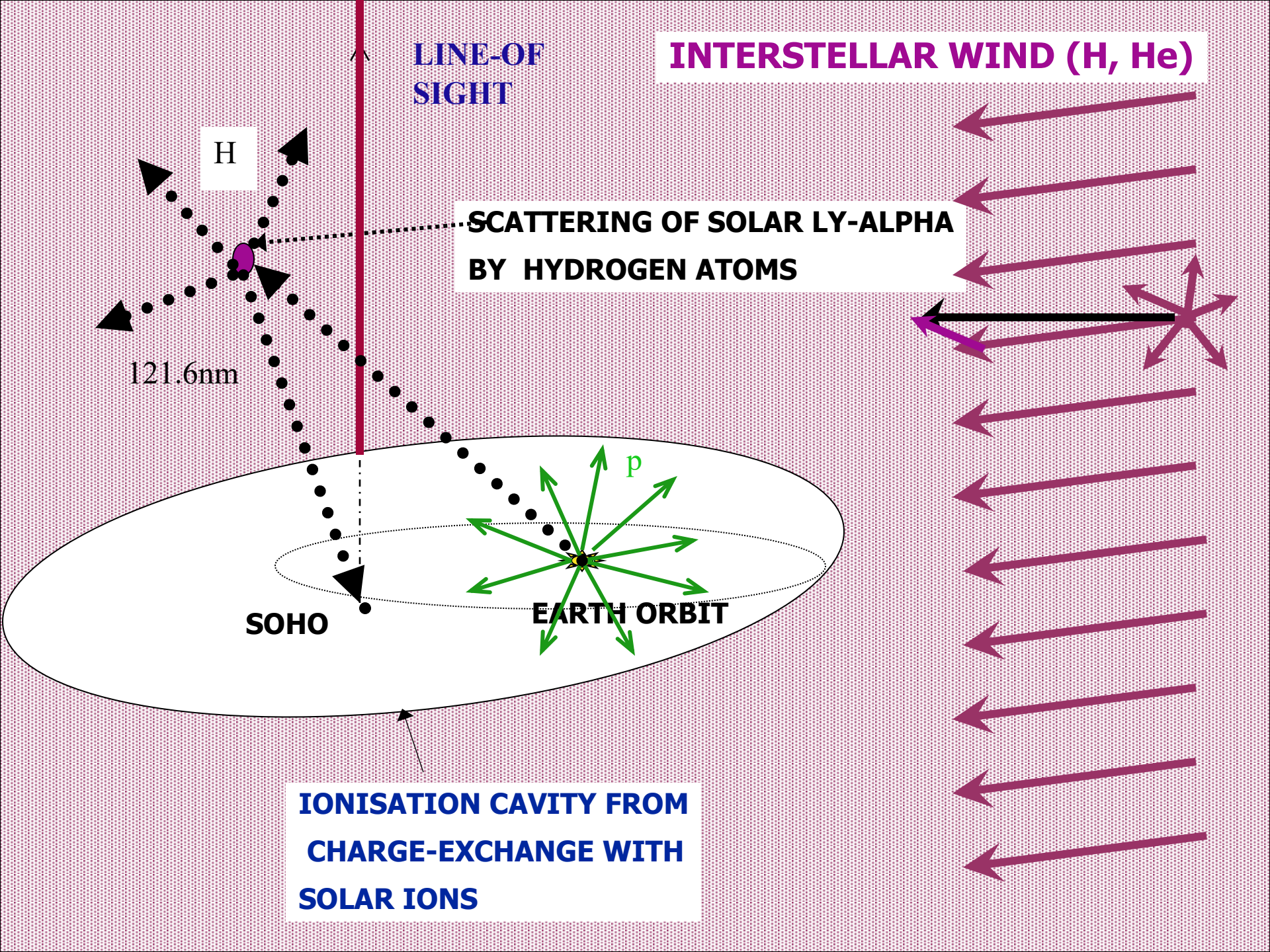
solar wind
 $\sim 400\text{--}700 \text{ km s}^{-1}$, $\sim 3\text{--}7 \text{ cm}^{-3}$ @ 1 AU
mostly proton

geocorona
 $\sim 25 \text{ cm}^{-3}$ @ 10 RE
mostly H atom



Along a given line-of-sight the contribution to the emission ends:

- either at the heliopause
- in the downwind direction where the particular solar ion has been entirely consumed



LINE-OF-SIGHT

INTERSTELLAR WIND (H, He)

H

SCATTERING OF SOLAR LY-ALPHA BY HYDROGEN ATOMS

121.6nm

p

SOHO

EARTH ORBIT

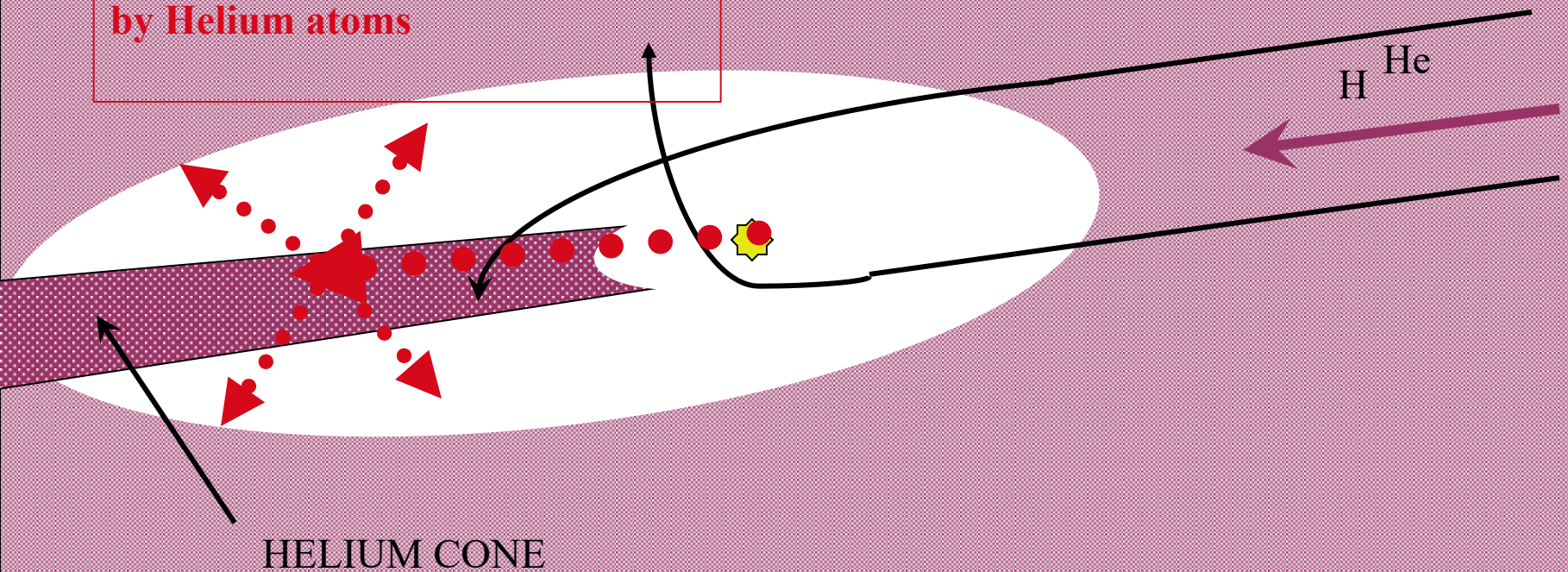
IONISATION CAVITY FROM CHARGE-EXCHANGE WITH SOLAR IONS

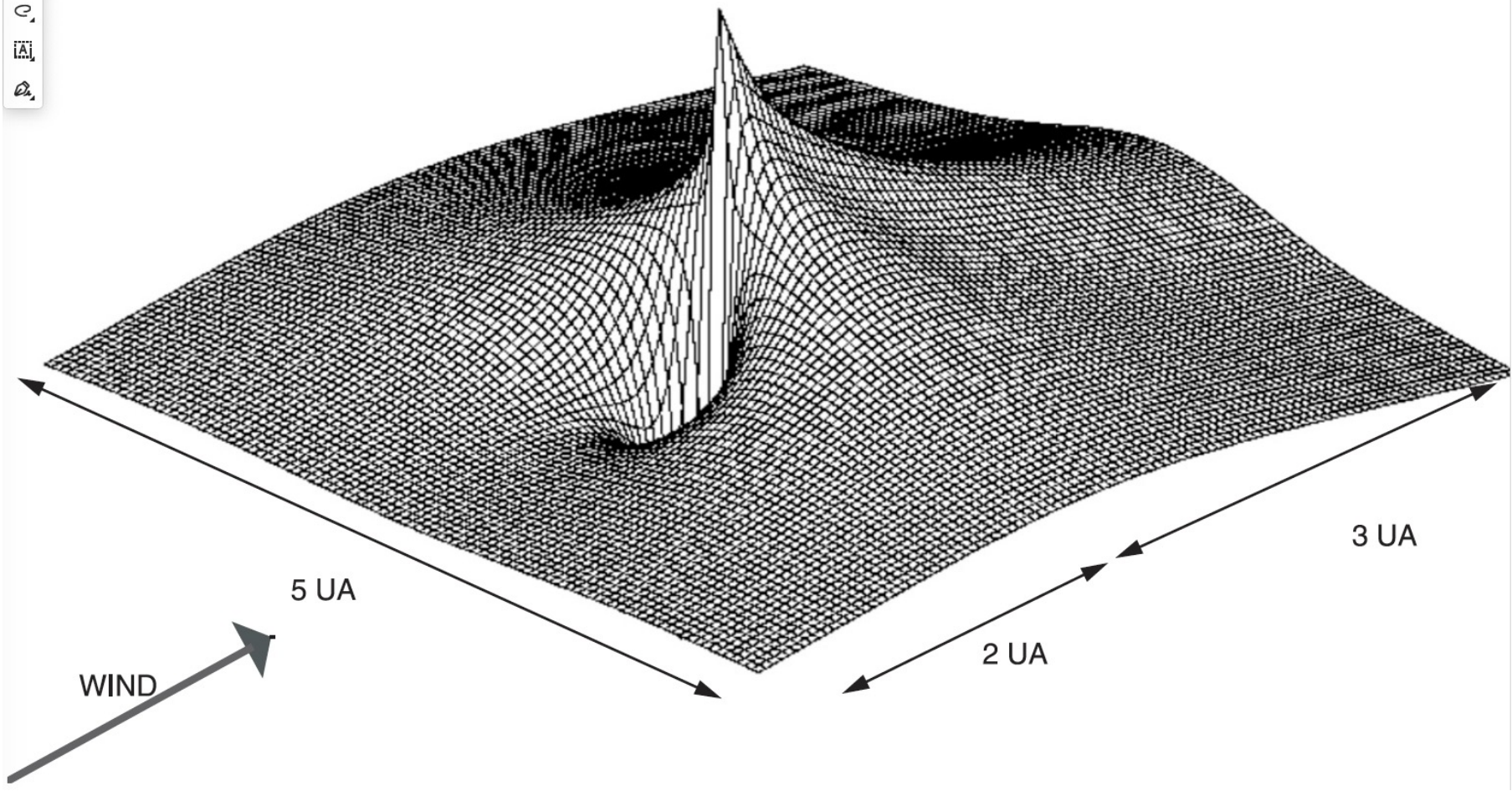
HELIUM

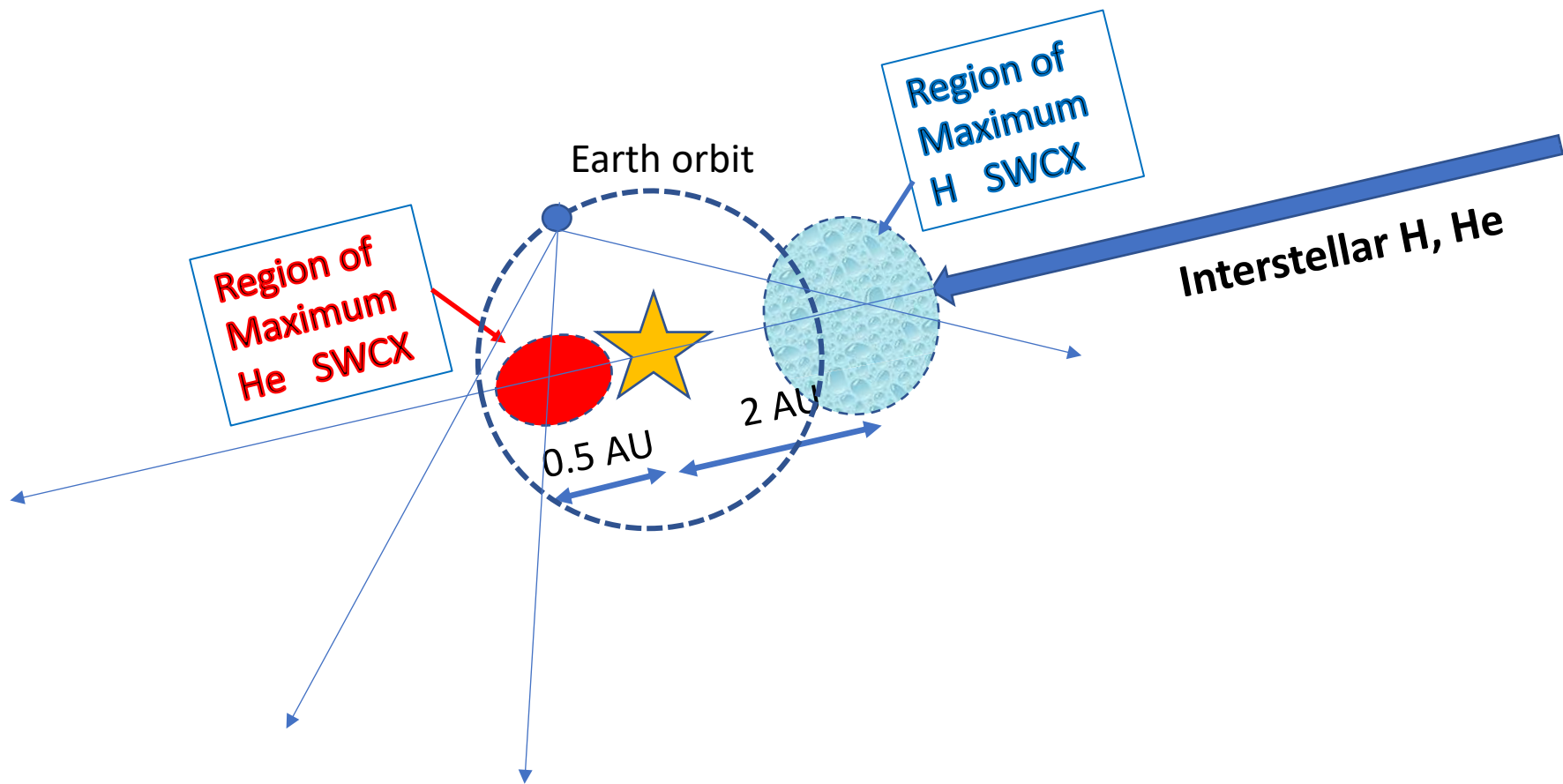
SMALLER IONIZATION

STRONG GRAVITATIONAL FOCUSING

SOLAR 58.4 nm photons
are resonantly scattered
by Helium atoms







**X-Ray Intensities
September 28 - October 24, 1990**

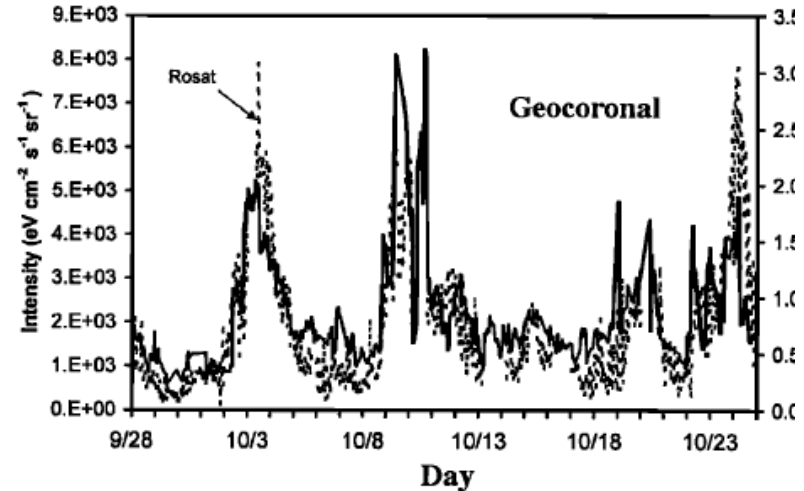
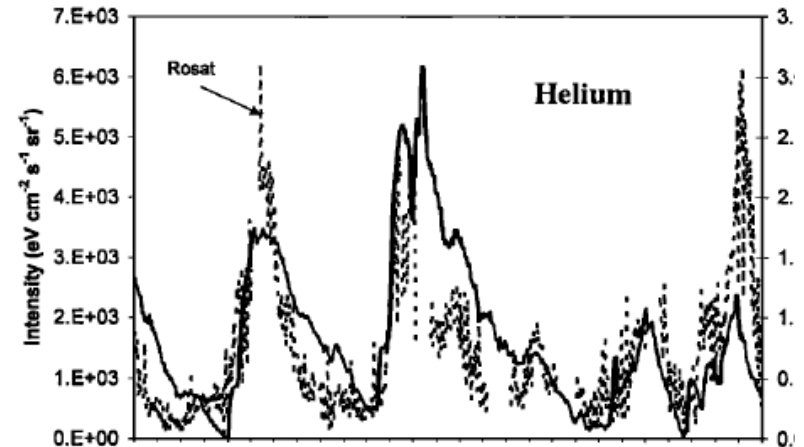
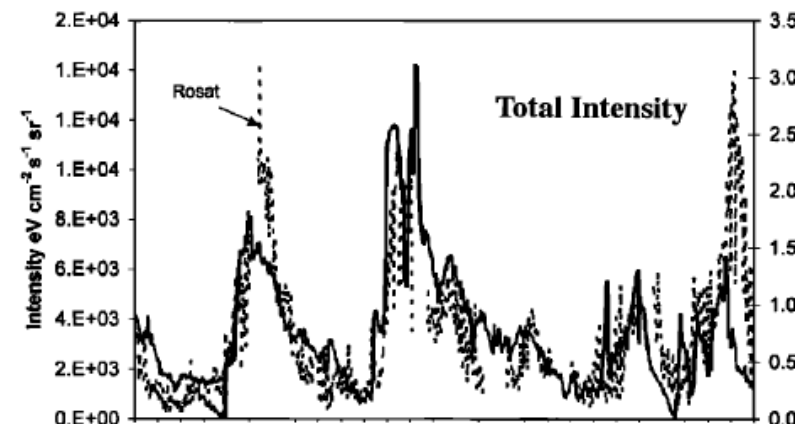
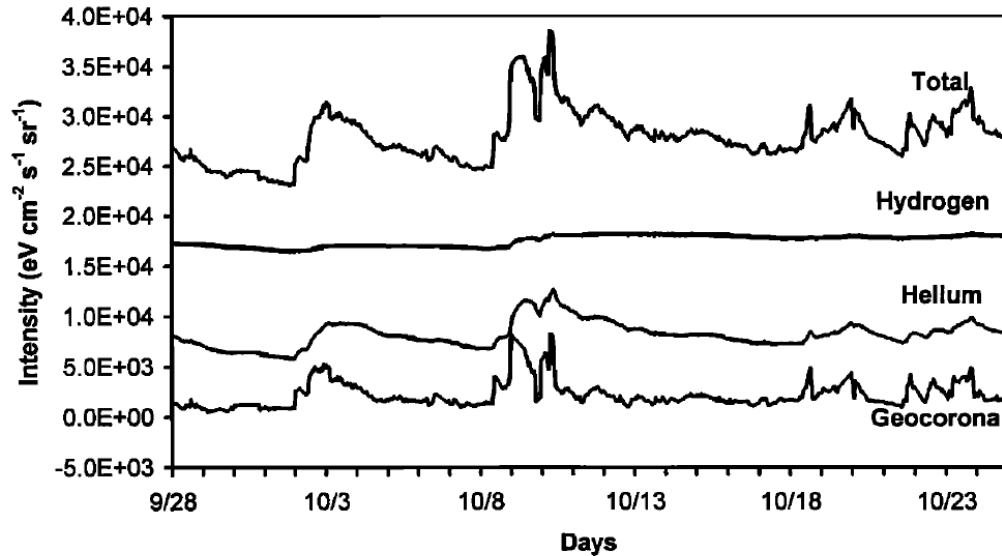


Figure 4. Model X-ray intensity versus time for the same time period as in Figure 3. Individual contributions from heliospheric H and He and from the geocorona are shown. The solar wind data used in the model included "interpolations" from other time periods (see text).

LATITUDINAL EFFECT



Solar maximum solar wind as measured by Ulysses/SWOOPS

Model description (1)

- density distribution of IS H and He atoms in response to the solar wind and solar EUV conditions for solar minimum and maximum activity.
- densities of heavy solar wind ions (X^{Q+}), modulated by collisions with the neutral heliospheric gas (a)

Along a SW
streamline

$$\frac{dN_{X^{Q+}}}{dx} = -N_{X^{Q+}}(\sigma_{(H,X^{Q+})} n_H(x) + \sigma_{(He,X^{Q+})} n_{He}(x)) + N_{X^{(Q+1)+}}(\sigma_{(H,X^{(Q+1)+})} n_H(x) + \sigma_{(He,X^{(Q+1)+})} n_{He}(x))$$

(a)

Loss term

Source term

Bare ion density & simplified case, loss term only:

$$N_{X^{Q+}}(r) = \frac{N_{X^{Q+0}}}{r^2} \exp\left(-\int_{r_0}^r (\sigma_{(H,X^{Q+})} n_H(x) + \sigma_{(He,X^{Q+})} n_{He}(x)) dx\right)$$

(b)

Model description (2)

- **self consistent** density grids of H and He neutral atoms and solar wind ions used to calculate the X-ray emissivity (d) due to the CX collisions

Volume collision
Frequency
($\text{cm}^{-3} \text{s}^{-1}$)

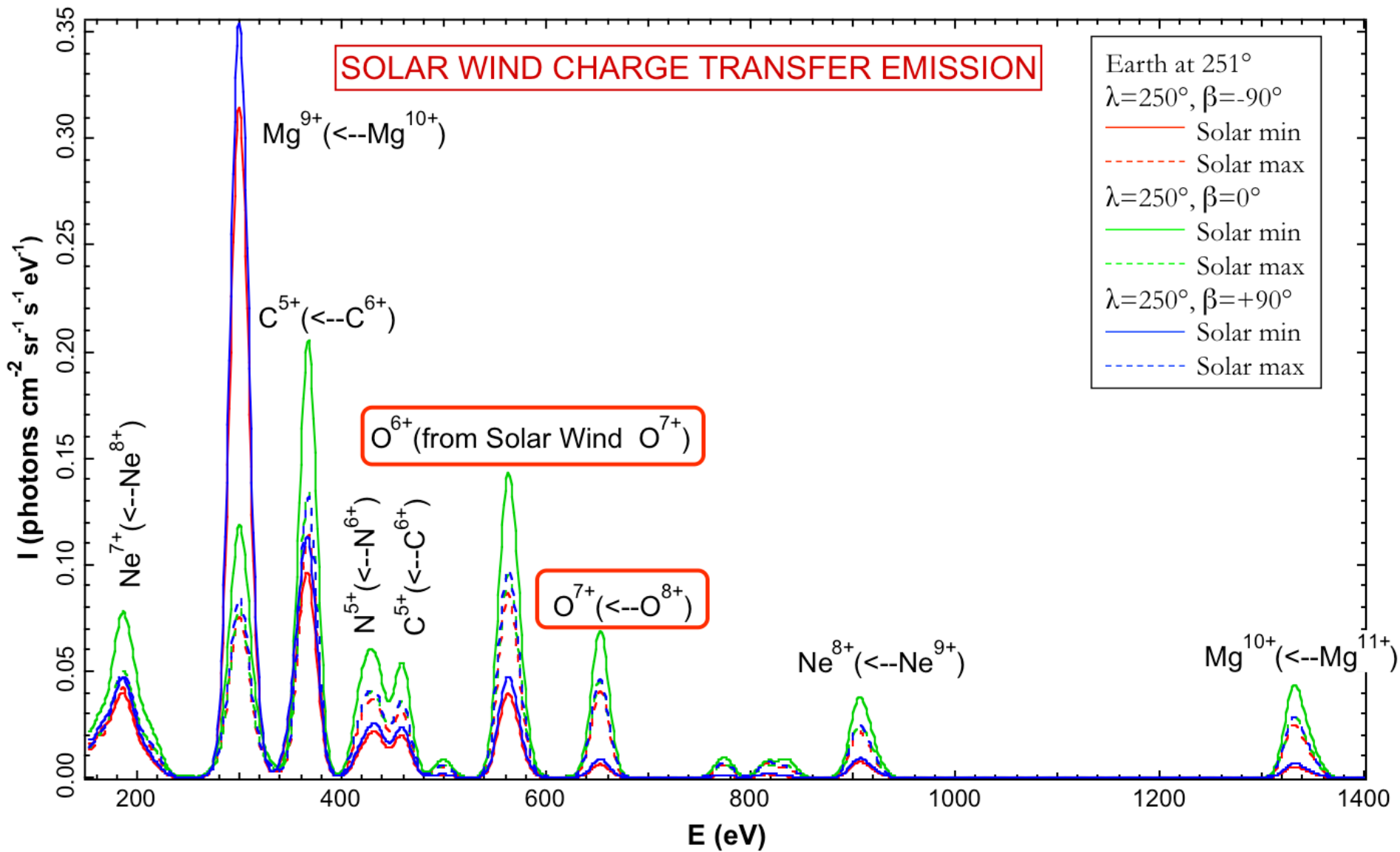
$$\begin{aligned} R_{X\varrho^+}(r) &= N_{X\varrho^+}(r) v_{\text{rel}} (\sigma_{(\text{H}, X\varrho^+)} n_{\text{H}}(r) + \sigma_{(\text{He}, X\varrho^+)} n_{\text{He}}(r)) \\ &= R_{(X\varrho^+, \text{H})}(r) + R_{(X\varrho^+, \text{He})}(r). \end{aligned} \quad (\text{c})$$

Emissivity
($\text{ph cm}^{-3} \text{s}^{-1}$)

$$\varepsilon_{h\nu}(r) = R_{(X\varrho^+, \text{H})}(r) Y_{(h\nu, \text{H})} + R_{(X\varrho^+, \text{He})}(r) Y_{(Eh\nu, \text{He})}. \quad (\text{d})$$

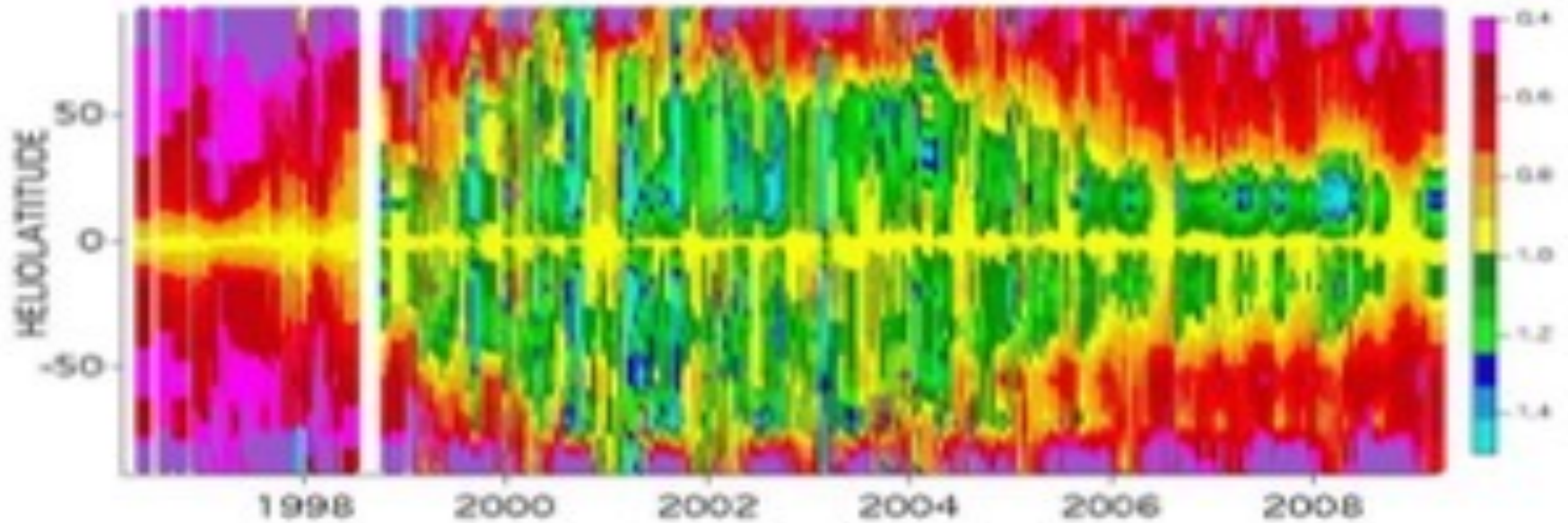
- total intensity along all lines of sight (e)

$$I_{h\nu}(\mathbf{O}, \text{LOS}) = \frac{1}{4\pi} \int_0^{\text{heliopause}} \varepsilon_{h\nu}(r) ds. \quad (\text{e})$$

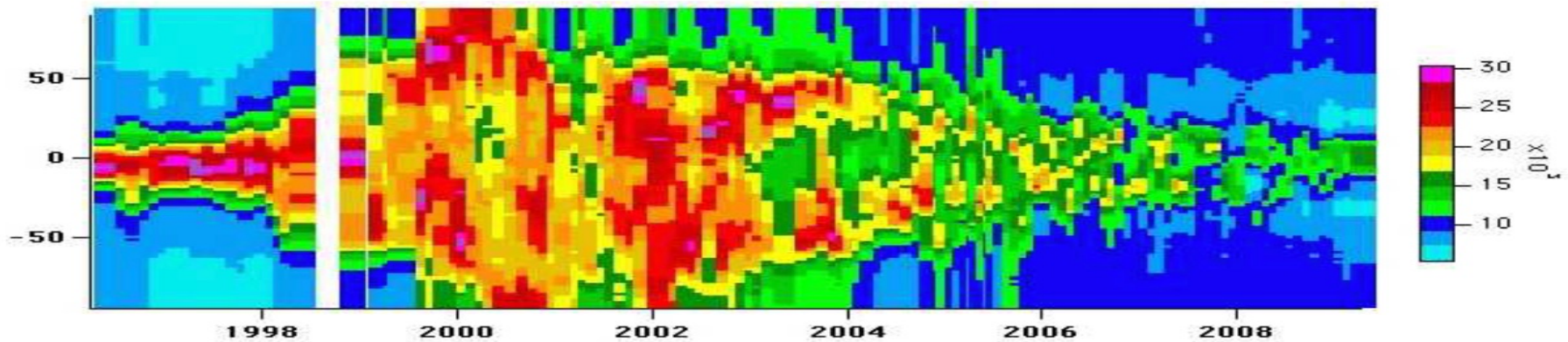


Koutroumpa et al., A&A, 2006

COMPLEX TIME DELAYS AND INTENSITY VARIATIONS DUE TO LATITUDINAL EFFECTS

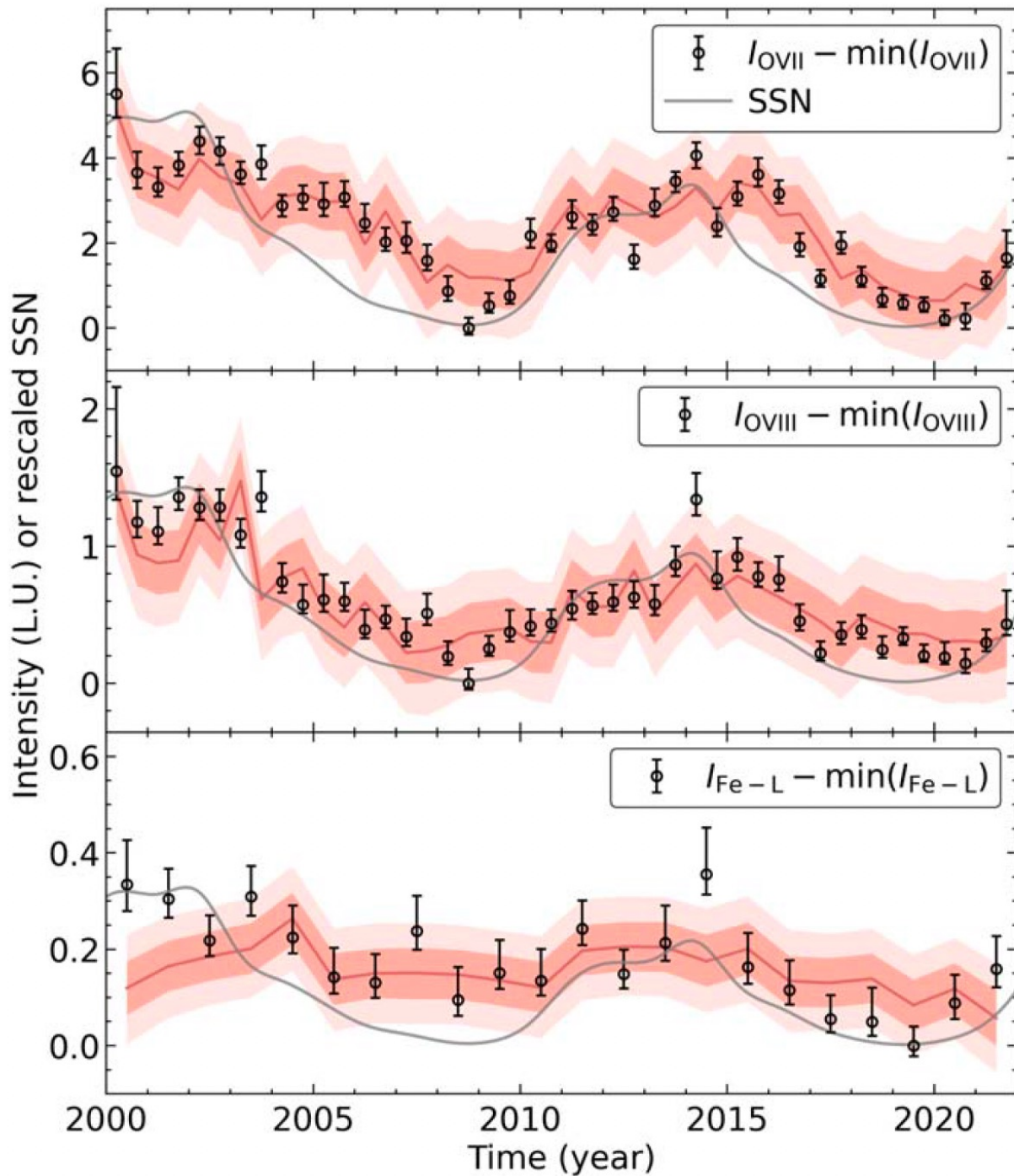


Interstellar H ionization rate at 1 AU as a function of time and heliolatitude (SOHO/SWAN)



CORONAL ELECTRON DENSITY (SOHO/LASCO/C2)

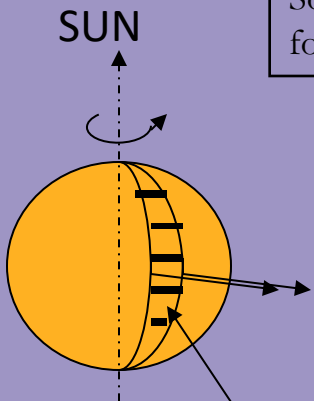
Signals out of phase in a complex way



XMM-Newton
archival data

Pan et al, 2024

Solar Wind enhancement localization
for $t=0$ d of observation



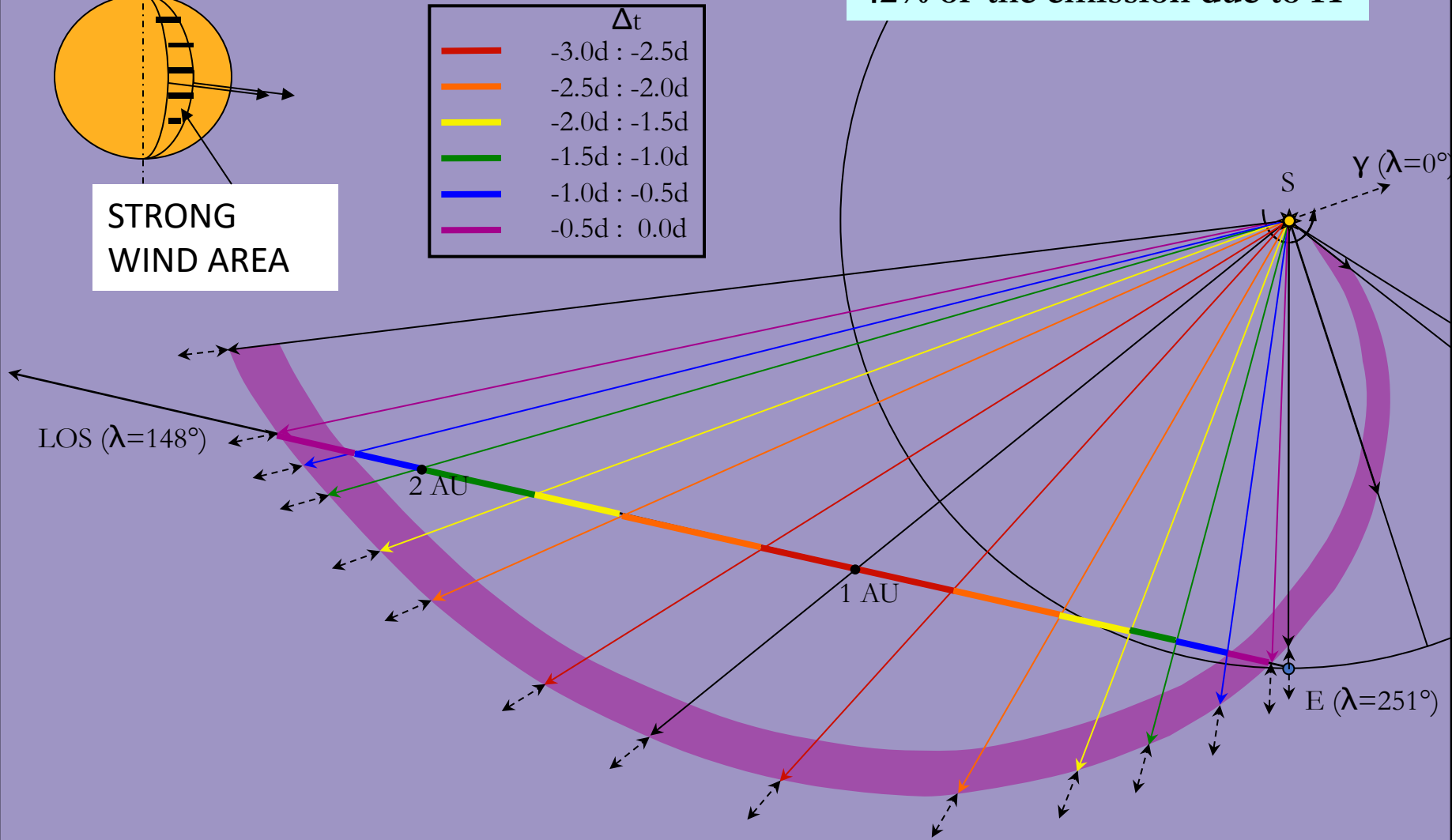
**STRONG
WIND AREA**

	Δt
	-3.0d : -2.5d
	-2.5d : -2.0d
	-2.0d : -1.5d
	-1.5d : -1.0d
	-1.0d : -0.5d
	-0.5d : 0.0d

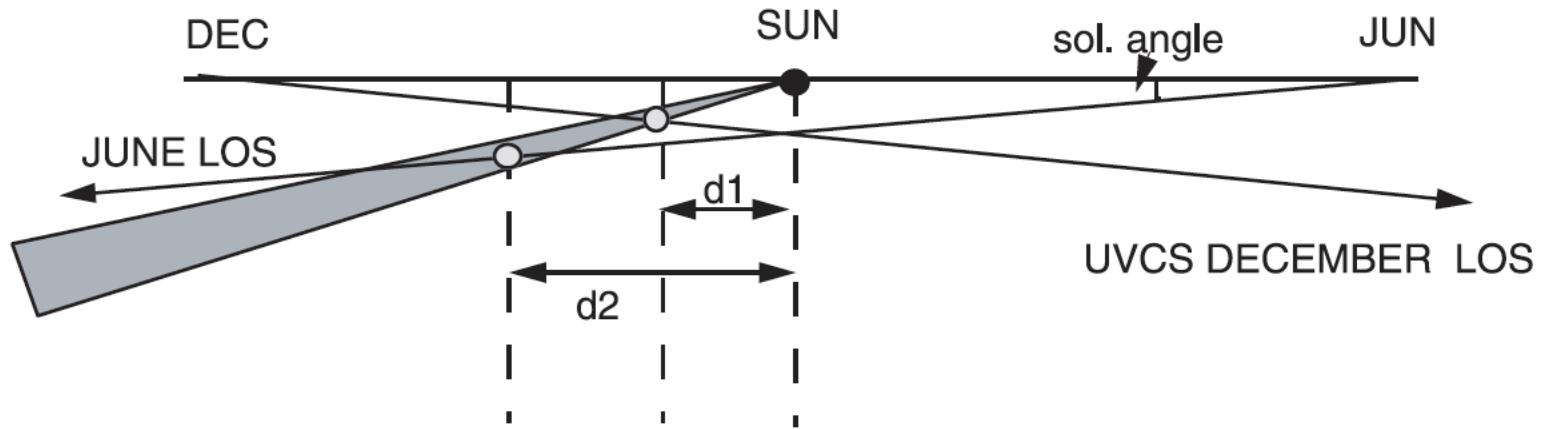
$D < 2$ U.A.:

88% of the emission due to He

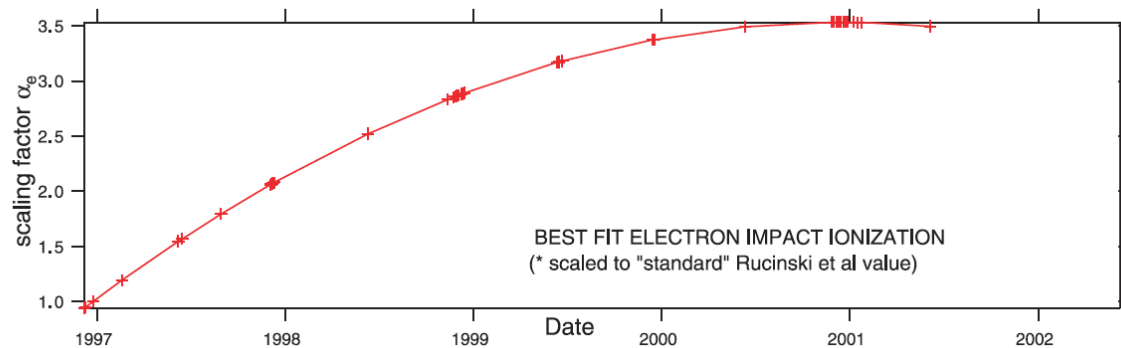
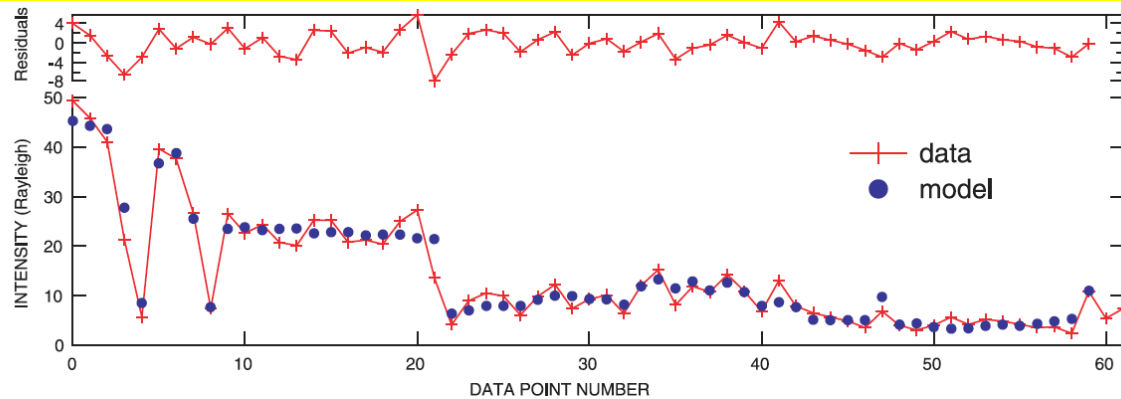
42% of the emission due to H

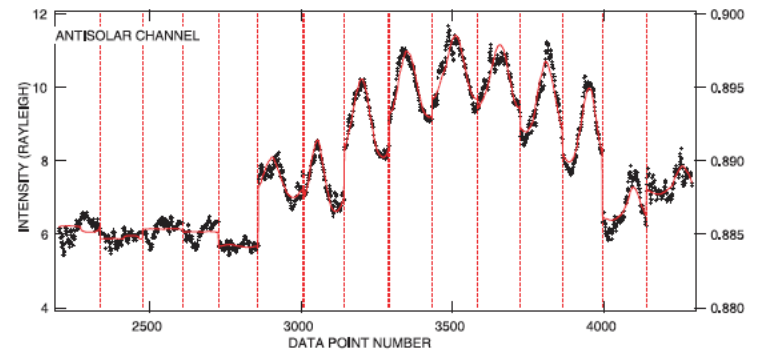
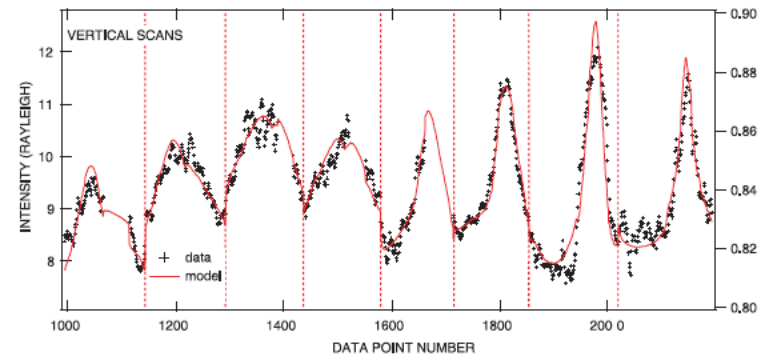
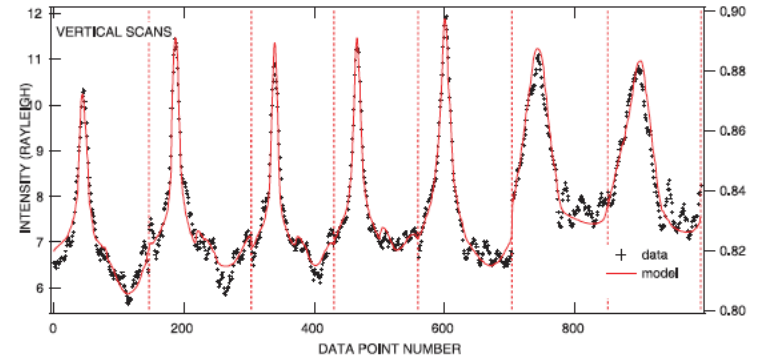
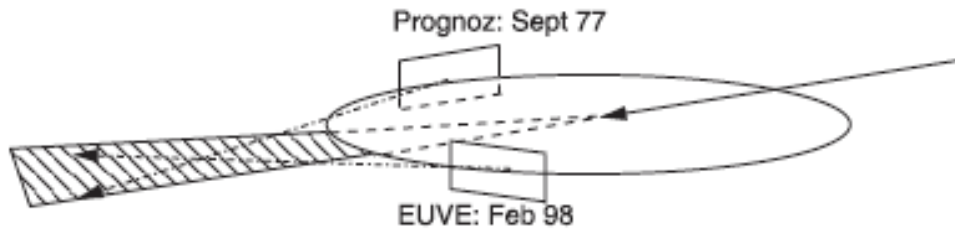


The very strong variability of the helium cone: electron impact ionization close to the Sun



Observations of the 58.4 nm diffuse emission (the helium glow) with SOHO/UVCS





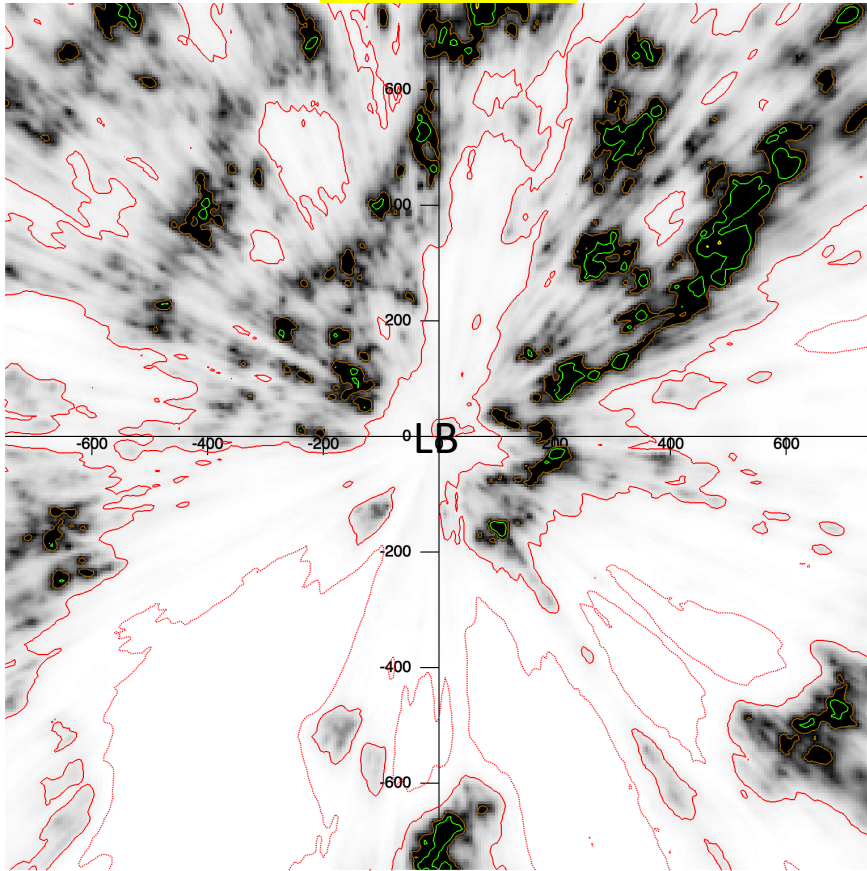
SWCX simulations for astronomical observations: all difficulties

- Different sources of neutrals
magnetosphere + heliospheric H, + heliospheric He
- and corresponding different solar wind propagation time
- Temporal evolution of the sources
- Need for Parker spiral for very strong SW events
- Strong variability of the Helium cone

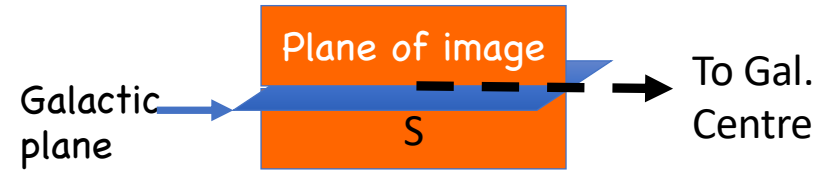
The trouble with the Local Bubble (LB)



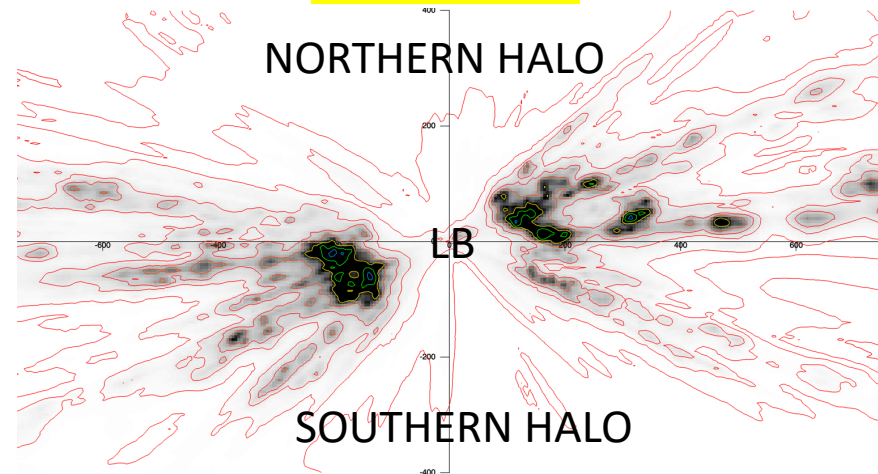
1500 parsec



Map with
5 pc covariance length

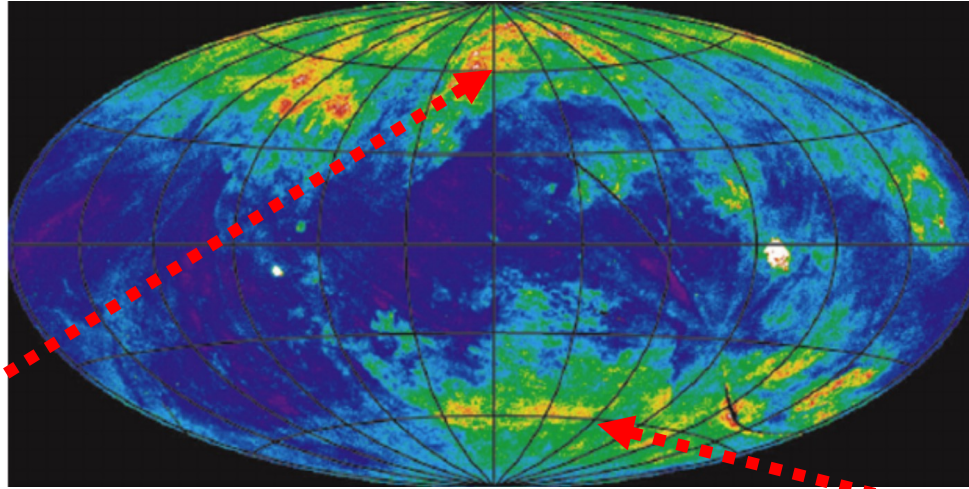


1500 parsec



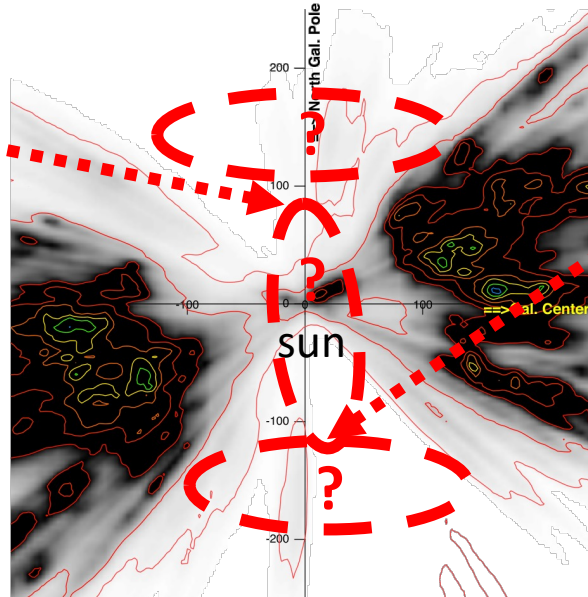
Vergely et al, 2022
maps and tools available
at explore-platform.eu

ROSAT ¼ keV map



Northern chimney

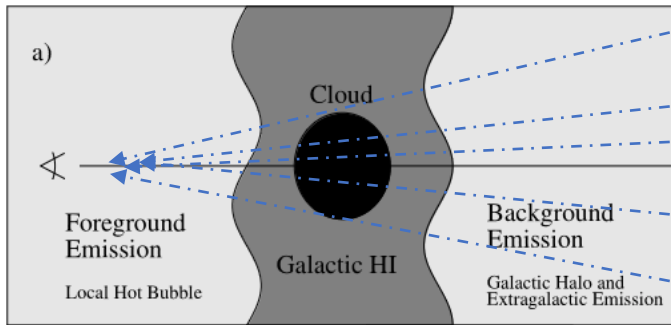
Southern chimney



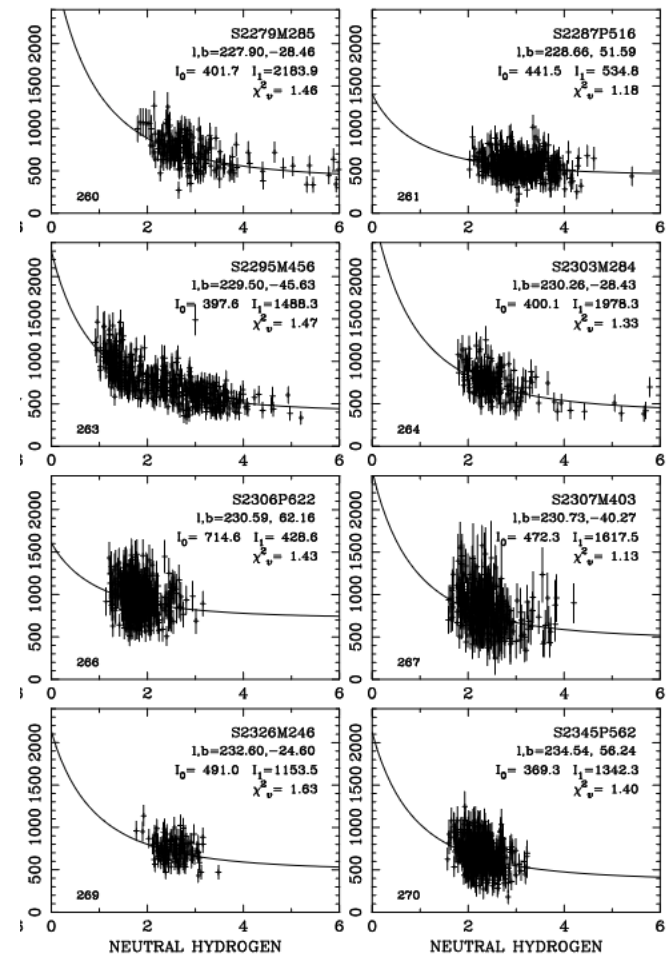
dust map in vertical plane

Is there hot gas X-ray emission only from the halo, or is there a contribution from the local bubble

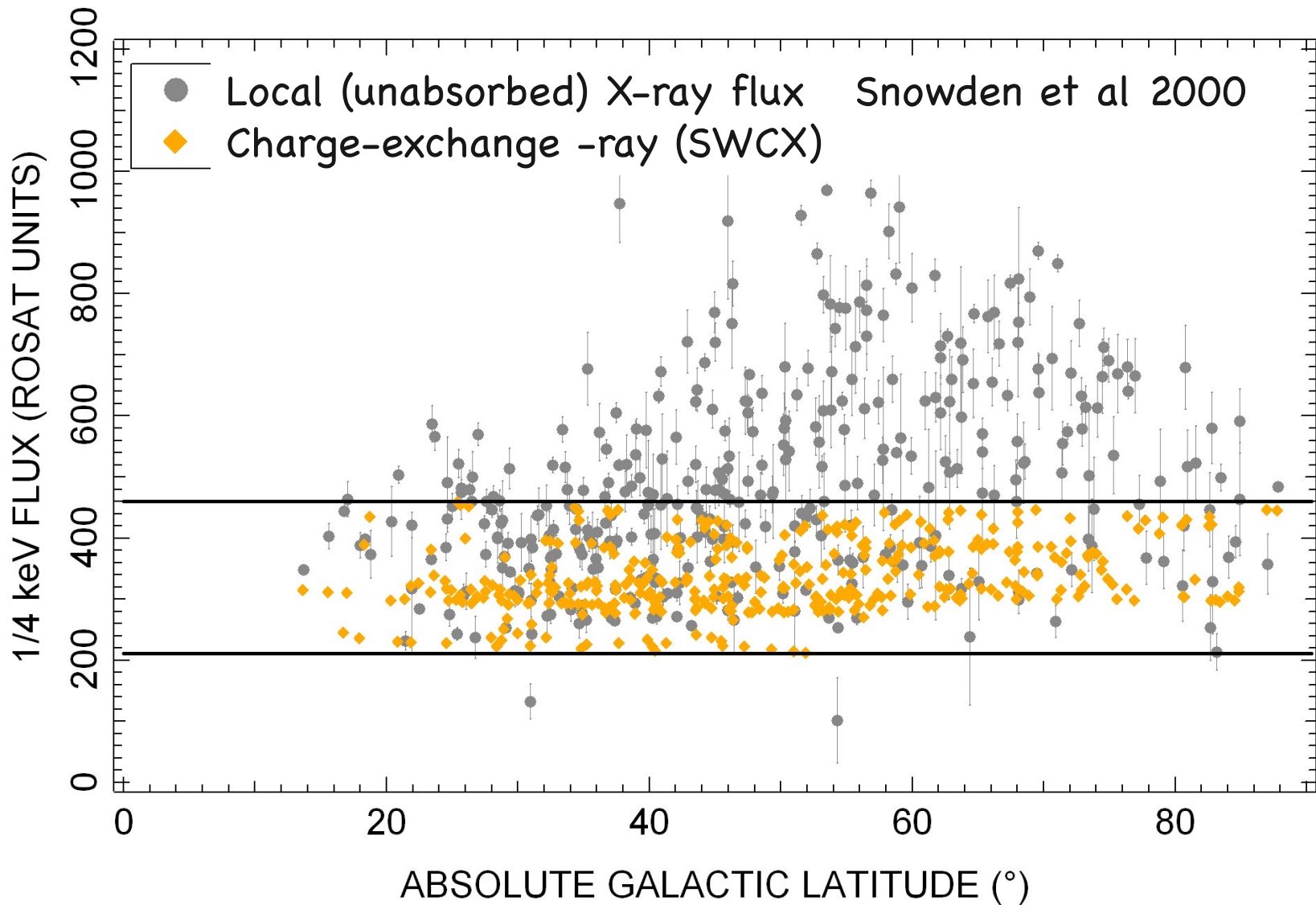
Using shadowing clouds to infer background and foreground emission (Snowden et al, 2000)



Authors used ROSAT $\frac{1}{4}$ keV (R12) and $\frac{3}{4}$ keV (R45) and DIRBE/IRAS 100 mm maps as a proxy for HI.

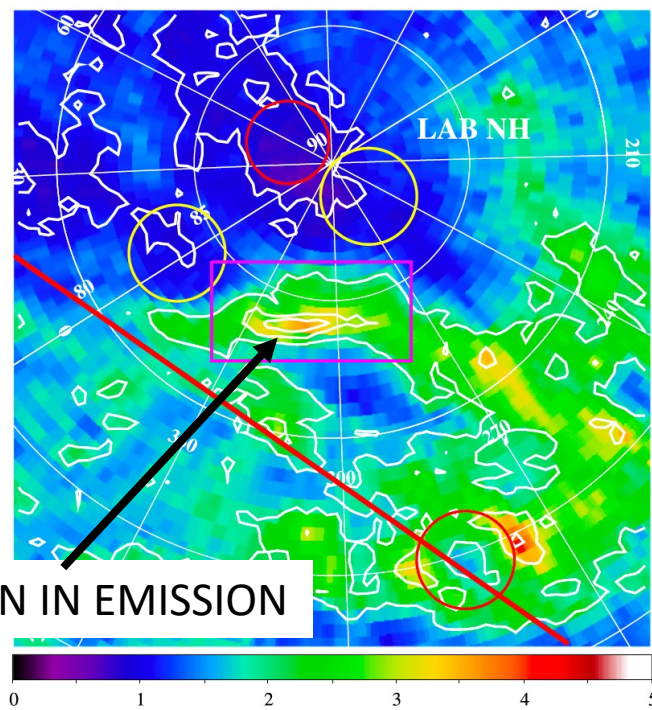
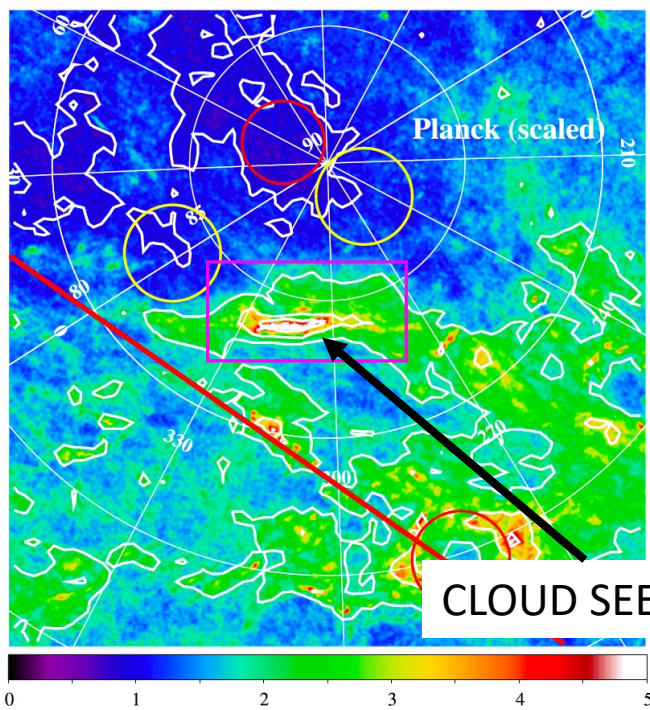


The foreground emission is due to the Local Bubble hot gas and to SWCX

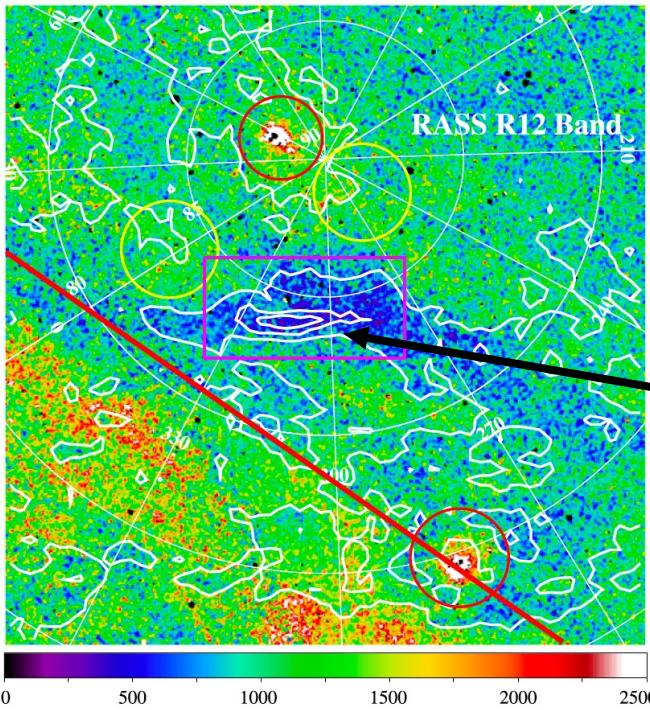


**R12 EMISSION FROM LOW LATITUDES ==
CLOSED TO SWCX**

DUST
EMISSION
(PLANCK)

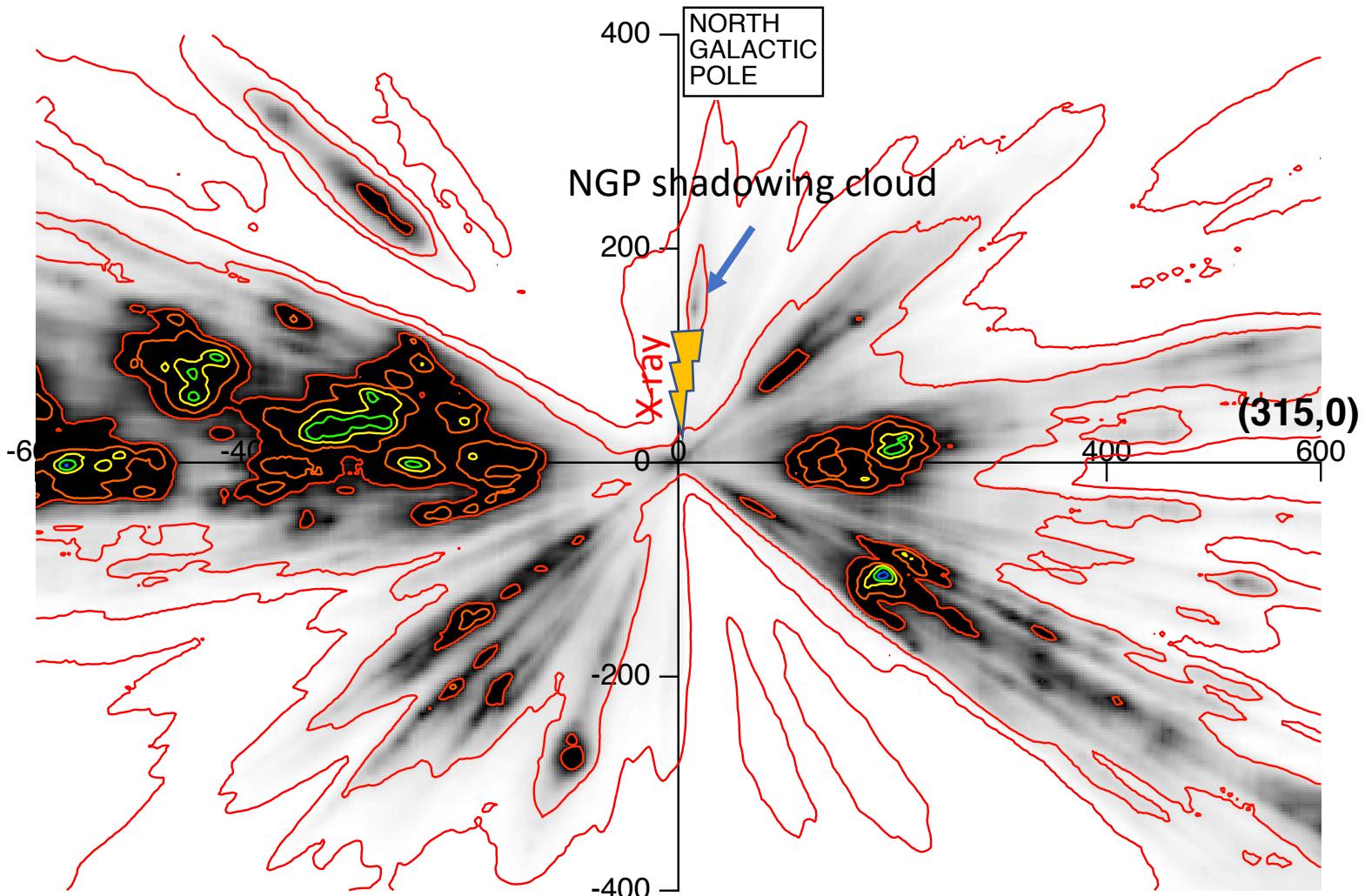



HI
EMISSION
21 cm



CLOUD SEEN IN ABSORTION
ROSAT R1/R2

Snowden et al, 2015



 = CX (magnetosphere) + CX (heliosphere) + Local Bubble hot gas
 50 131 217 Rosat Units

Series of shadowing experiments= > there is hot X-ray emitting gas in the local bubble!

CXU

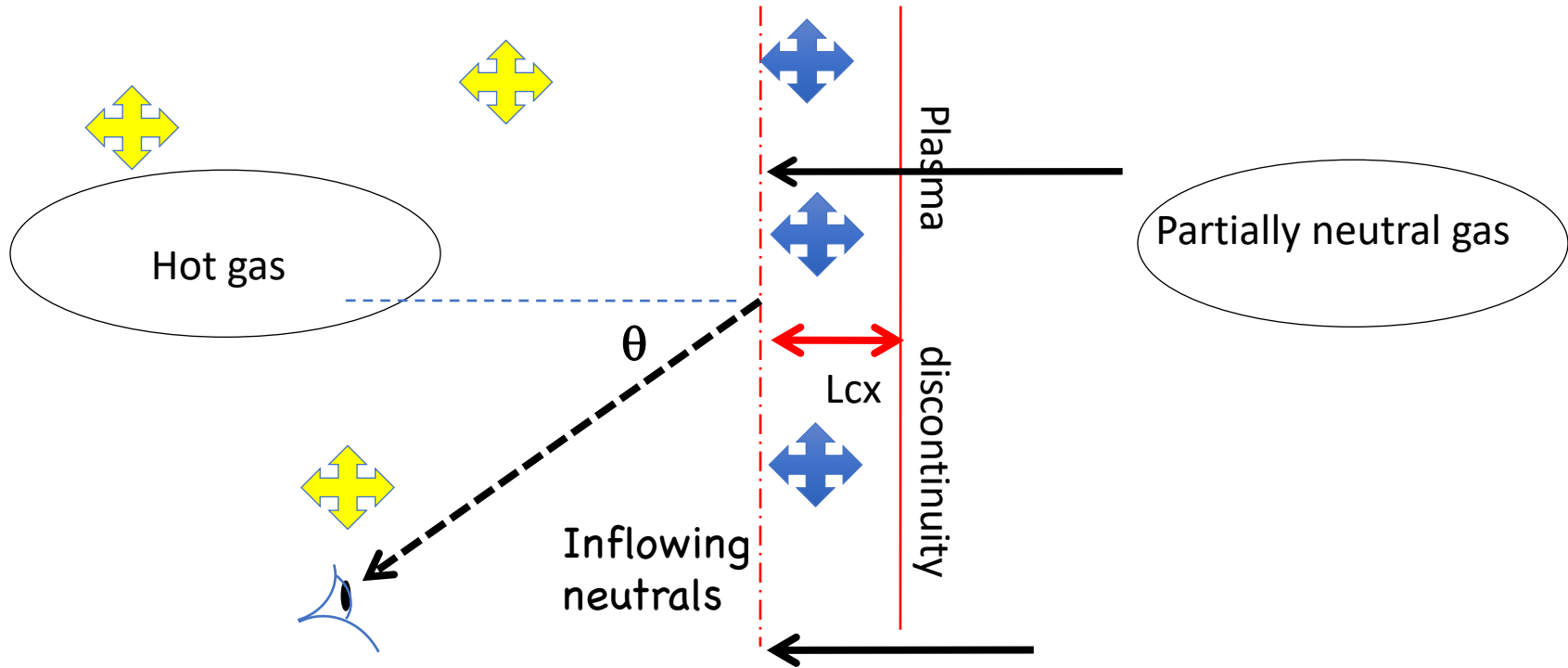
-for a broad view see the very exhaustive review of Gu and Shan (2023) !!!

Question: The **solar wind** is the CX favourable case of a **cool plasma with « frozen » charge-state of the ions** => neutrals entering the solar wind **do not suffer from collisional ionization with electrons** and **there is no hot gas thermal X-ray**.

It may be the case of astrospheres , or expansion of hot gas in quasi-vacuum.

This is not the case for interfaces between **hot gases and cool partially neutral gas**.
What happens then?

CTX emission arises in narrow layers that correspond to the mfp of neutrals against ionization

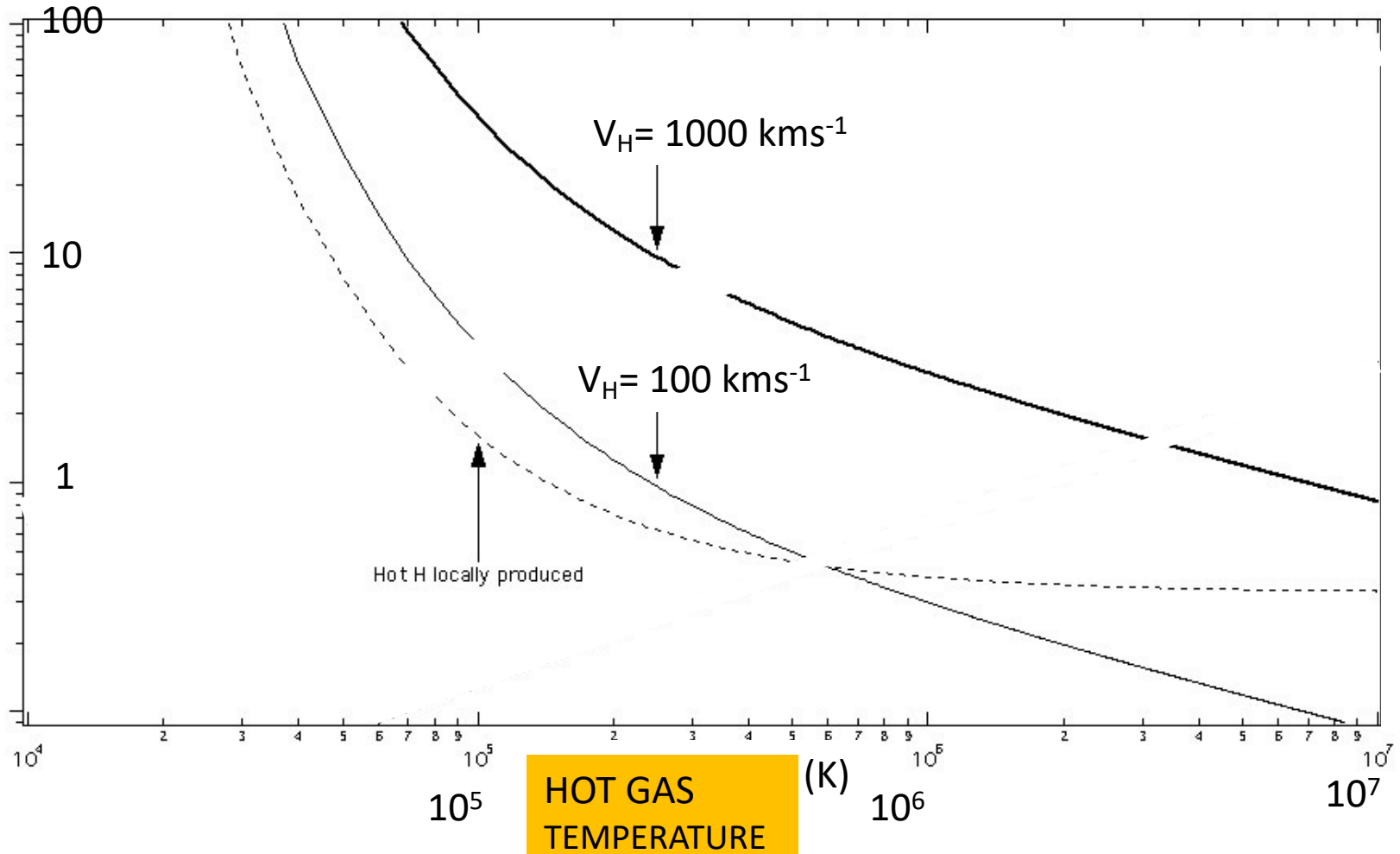


L_{cx} = mfp of neutrals through the hot gas

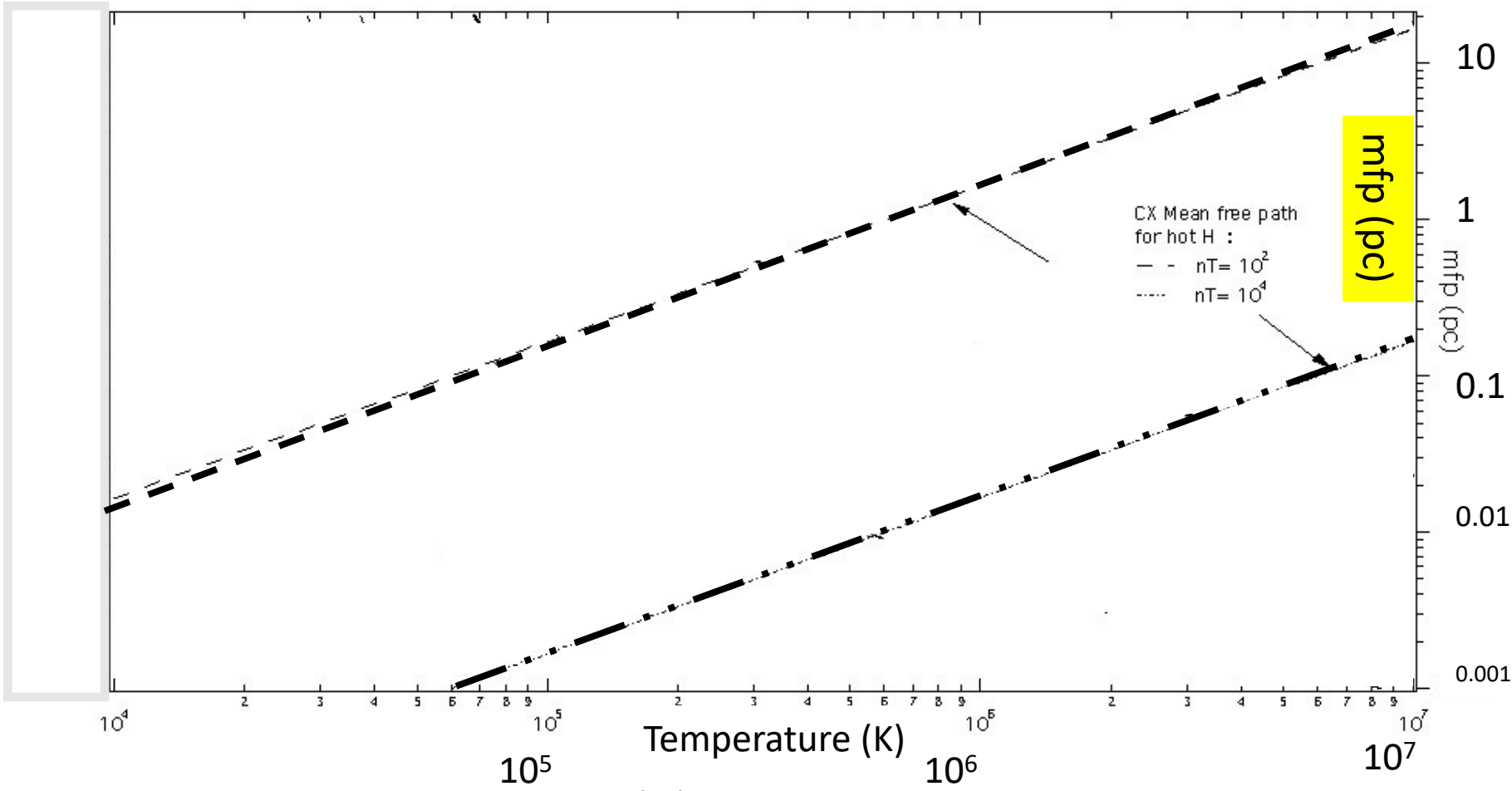
Absolute emission unimportant: what matters is the relative intensity of the CTX () w.r.t. the hot gas emission ()

Neutral H atoms « launched » in hot gas
CHARGE-TRANSFER vs COLLISIONAL IONIZATION

H/H+ CX rate/ e ionization rate

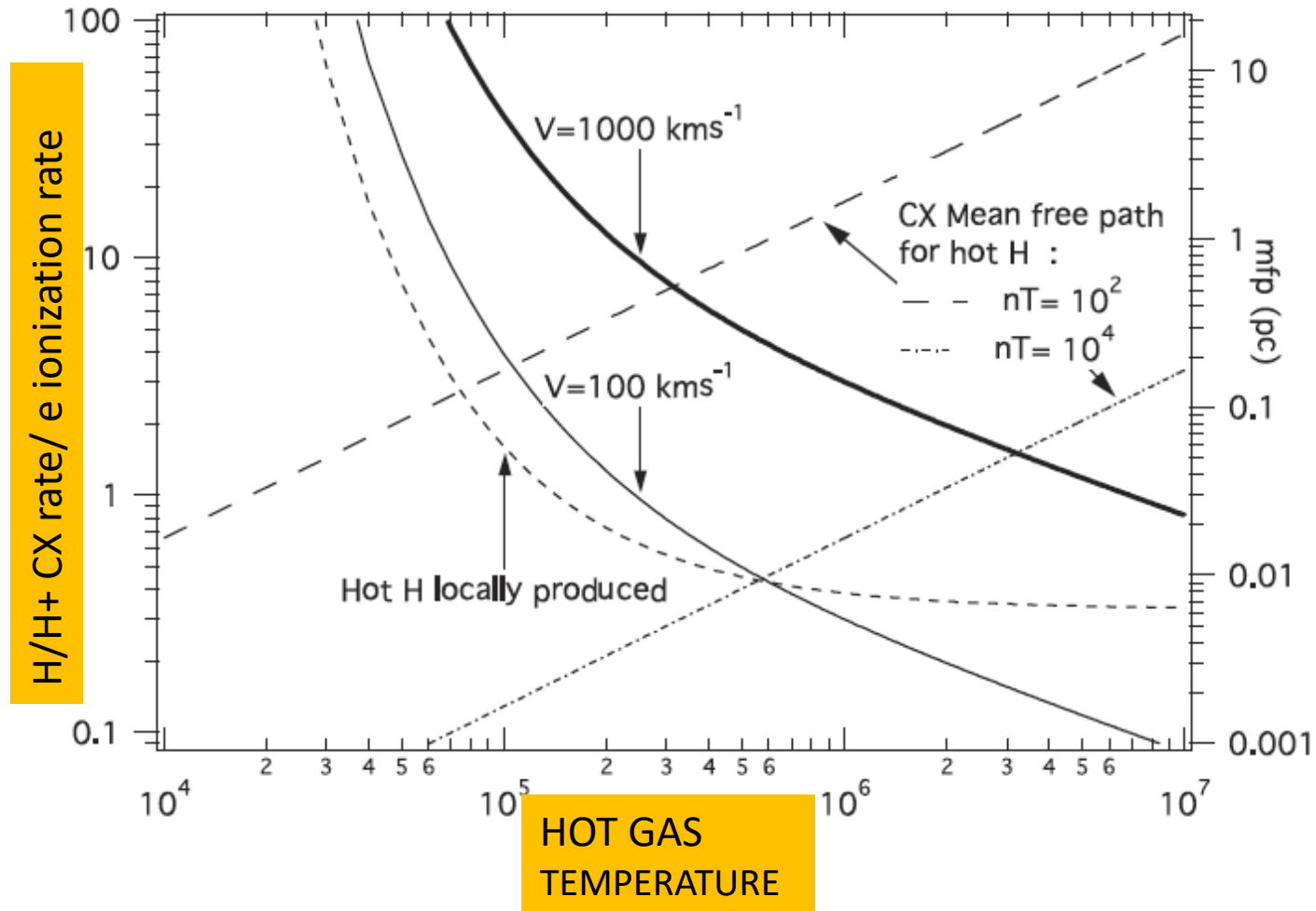


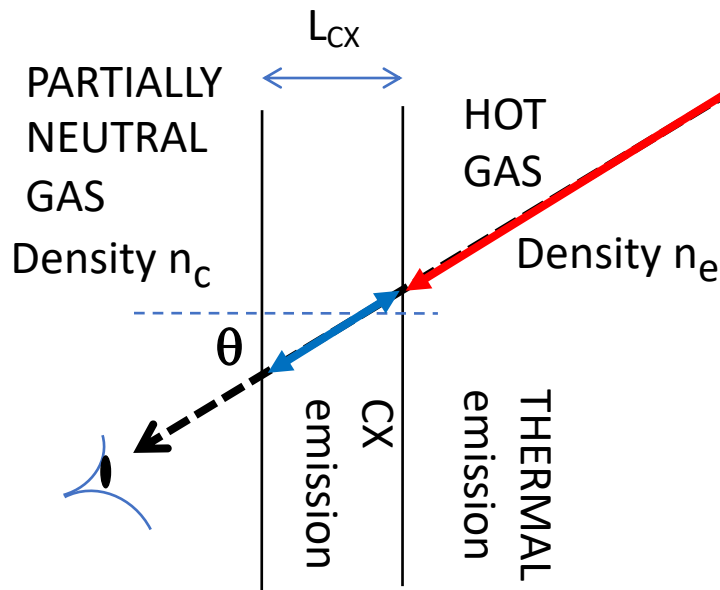
Neutral H atoms « launched » in hot
Mean free path against ionization



Ionization of an H atom launched in hot gas

CX ionization vs electron impact ionization





What counts is the ratio between the CX emission (from the narrow layer) and the thermal emission from the hot gas

One way to estimate the potential importance of the CX layer is to convert it into an equivalent path of hot gas thermal emission, and compare with the size of the path through the hot gas

$$L_{pc} = 3 \times 10^{-2} \left(\epsilon \alpha \chi_{T,a}^{-1} \right) \left(n_c V_{100} n_e^{-2} \right)$$

V_{100} : hot/cold gas relative velocity in units of 100kms⁻¹

L varies as n_e^{-2}

ϵ = fraction of neutrals experiencing charge transfer before being collisionally ionized

α = hot gas metallicity/ solar ($\alpha = 1$ for solar)

χ = hot gas emissivity/ (T=10⁶ K, $\alpha = 1$) gas emissivity

E.g. L on the order of 100 kpc if $n_c = 0.1 \text{ cm}^{-3}$, $n_e = 10^{-4} \text{ cm}^{-3}$
 T hot= 10⁷ K, T cold=10⁴ K (filament in galaxy cluster gas)

Approach used by Katsuda et al, 2011 for the Cygnus loop

Another view:

Estimates of CX in cluster filaments (Fabian et al, 2011)

-1) assumes that **hot gas penetrates the cooler filamentary gas through reconnection diffusion** reconne

-2) ions and H⁺ neutralized by H,He in proportions similar to their abundances

Fabian et al, 2011 conclude in negligible CX intensity, while Walker, Kosec, Fabian et al, find the spectra compatible with CX significant contribution

Diagnostics for CXU

SPECTRAL

Helium-like ions triplet: forbidden line relative increase

$$G=(f+i)/r >2$$

$Ly\beta/Ly\alpha$ and in general High-n shells enhancements

anomalous abundances

CX = lines only => \neq continuum to line ratios (at high T)

SPATIAL

emission from filamentary, sheet-like structures

tight correlation with H-alpha

unexpected emission, overcomes shadowing due to clouds

correlation of spectral properties with presence of clouds

The CXE brightness varies as $n_e \cdot n_h \cdot V_{rel}$

The hot gas thermal emission brightness varies as n_e^2

The relative importance of the increases when the hot gas density decreases

Crucial need for high-resolution spectroscopy !!!

XRISM: please open the door !

